NONLINEAR OPTIMAL CONTROL AND NEAR-OPTIMAL GUIDANCE STRATEGIES IN SPACECRAFT GENERAL ATTITUDE MANEUVERS

by

Yiing-Yuh Lin

Dissertation submitted to the Faculty of the
Virginia Polytechnic Institute and State University
in partial fulfillment of the requirements for the degree of
DOCTOR OF PHILOSOPHY
in
Engineering Mechanics

APPROVED:

L. G. Kraige, Chairman

C. W. Smith

A. H. Nayfeh

S. L. Hendricks

H. F. VanLandingham

July 1988

Blacksburg, Virginia

NONLINEAR OPTIMAL CONTROL AND NEAR-OPTIMAL GUIDANCE STRATEGIES IN SPACECRAFT GENERAL ATTITUDE MANEUVERS

by

Yiing-Yuh Lin

L. G. Kraige, Chairman

Engineering Mechanics

(ABSTRACT)

Solving the optimal open-loop control problems for spacecraft large-angle attitude maneuvers generally requires the use of numerical techniques whose reliability is strongly case dependent. The primary goal of this dissertation is to increase the solution reliability of the associated nonlinear two-point boundary-value problems as derived from Pontryagin's Principle. Major emphasis is placed upon the formulation of the best possible starting or nominal solution. Constraint relationships among the state and costate variables are utilized. A hybrid approach which begins with the direct gradient method and ends with the indirect method of particular solutions is proposed. Test case results which indicate improved reliability are presented.

The nonlinear optimal control law derived from iterative procedures cannot adjust itself in accordance with state deviations measured during the control period. A real-time near-optimal guidance scheme which takes the perturbed states to the desired manifold by tracking a given optimal trajectory is also proposed. Numerical simulations are presented which show that highly accurate tracking results can be achieved.

ACKNOWLEDGMENTS

The author would like to express his deep appreciation to his advisor, Dr. L. Glenn Kraige, for his suggestions, criticisms, and unending editorial assistance during the course of this research project. Without his help and support, it is doubtful that this work could have ever been completed. The author also wishes to express his thanks to his advisory committee, Drs. Hendricks, Nayfeh, Smith, and VanLandingham, for their contributions to his education and their willingness to review his dissertation. Thanks also goes to Dr. Frederick, Department Head of Engineering Science and Mechanics, for providing financial support. The work done by previous researchers at VPI&SU is also acknowledged.

Special thanks is also given to the author's parents

for their encouragement and constant support. Most of all, the author is grateful to his wife and two children for their patience, understanding, sacrifice, and the joy they bring to the author's life.

TABLE OF CONTENTS

LIST OF TABLES

LIST OF FIGURES

CHAPTER 1

INTRODUCTION

Not until the mid-twentieth century did the development of optimal control theory and its applications begin to advance in parallel with computer technology. Applying optimal control theory, which is an extension of the calculus of variations, to regulate a dynamic system always results in a boundary-value problem with constraint conditions specified on at least two points of the motion trajectory. Only for some special cases can analytical solutions be formulated. Most of the time the problems must be solved through numerical procedures, which, even for relatively simple problems, are impractical to carry out by hand. This is why, over a period of some two hundred years, the calculus of variations was a playground of mathematicians, attracting little attention from engineers. The advent of the computer has made possible the development of numerical strategies for solving optimal control problems with manageable time and cost.

Employing optimal control strategies to spacecraft attitude maneuvers has attracted an increasing number of investigations. Solving the problems of optimal attitude control of rigid spacecraft is the interest of this research. This special class of problems is important in its own right and as a starting basis for solving more general attitude maneuver problems such as those for spacecraft with flexible structures. Also, many of the ideas can be carried over to treat other dynamical problems as well.

The control problem for the spacecraft attitude motion consists of a set of nonlinear ordinary differential equations with boundary conditions at a specified initial time and at a fixed or free final time. The actual application may be the proposed

large space telescope, which requires that very precise control of an inertially-fixed attitude be maintained for long periods of time, followed by a large reorientation prior to examining the next celestial object. Earth-scanning spacecraft present the different problem of reorientation maneuvers between periods of remaining earth-pointing. In the case of various tracking spacecraft, the problem might be one of quickly aiming at a moving target.

Several active control mechanisms are currently available for spacecraft attitude maneuvers. Among the most commonly used are external thrusters, reaction wheels, control moment gyroscopes, and magnetic coils. Control efforts generated from external thrusters are by expelling propellant, while those from reaction wheels are by altering their angular speeds with electric motors. Control moment gyroscopes are rapidly spinning wheels whose axes may be reoriented relative to the spacecraft. Magnetic coils also use electric current to produce magnetic dipole moments which interact with the earth's magnetic field to produce torques. Some attitude control systems consist of a combination of the aforementioned control devices. In general, external thrusters, used to generate large torques, and reaction wheels, for small torques, are popular in spacecraft attitude control because they are easy to design and implement [1].

Small-angle attitude control maneuvers of rigid spacecraft can be treated by linear optimal regulator theory, while large-angle optimal rotational maneuvers so far have no standard solution method. Due to the nonlinearity of the system equations associated with large-angle rotation, the optimal attitude control problem as derived from Pontryagin's Principle or the calculus of variations is a nonlinear two-point boundary-value problem (NTPBVP) consisting of twice the number of equations as in the original system with split boundary conditions. An iterative or numerical method

is generally required to solve the problem. Although a complete closed-loop feedback control is desirable, it is difficult to formulate. As the constrained differential equations are coupled nonlinear equations, some linearization and transformation techniques are needed to approximate the closed-loop transition matrix, and they may be only applicable to some special cases [2-7].

Of all the available computing methods, no single solution technique can solve most of the optimal spacecraft attitude control problems. A number of algorithms for solving large-angle fixed-final-time maneuvers have been proposed [8-14]. Junkins and Turner [8] presented a relaxation procedure to solve problems with unconstrained external torque controls. Skaar and Kraige [9] used the same approach for the problems with unconstrained and constrained control torques generated by reaction wheels. The procedure, summarized as a differential correction algorithm similar to that of Reference [10], begins by linearizing state-costate equations about a closed-form single-axis solution. Then through the correction of initial costates by minimizing an augmented final-state errors function with respect to the change of initial costates, the initial costates are updated and a solution is found when the value of errors function is less than a small preset positive number. Vadali [11] applied the method of particular solutions for problems with external thrusters and internal reaction wheels. The maneuver trajectory is found by linearly superimposing a set of particular solutions, which were generated by directly integrating the quasilinearized state-costate differential equations. The difficulty encountered with the methods used in [8-10] is to provide a fairly good initial estimate of the unknown initial costates or motion trajectories. Hales, Flügge, and Lange [12] used a discrete steepest-descent method to solve for minimum-fuel attitude control problems with constrained external thrusters. Transforming the integral cost functional into a summation and guessing the switching times of the control trajectory, they applied a

steepest-decent technique to find a train of pulse-like control solution. The minimum-fuel attitude control problem was also treated by Wolske [13] by a linear programming strategy, and an approximate optimal trajectory was derived. Thompson [14] applied the method of asymptotic perturbation, which numerically perturbs the differential equations, but showed little or no practical application to the large-angle maneuver.

The solutions for improving the optimal attitude control strategy of rigid spacecraft have been identified in the above review of existing work and are now summarized. The failure of numerical methods for solving the NTPBVP usually stems either from a poor initial guess of the optimal solution, which causes the iteration to diverge, or from an overly slow convergence rate. One of the objectives of this research is to improve the solution reliability of the NTPBVP associated with nonlinear optimal attitude control of rigid spacecraft. Two approaches are proposed to increase the convergence rate and reduce the number of iterations of numerical methods. The first approach is the development of a systematic way to design a good initial nominal solution. The second is to combine two different methods, one with low sensitivity to the initial guess but a slow final convergence rate and the other with a fast final convergence rate but high sensitivity to the initial guess. Such a hybrid technique utilizes their advantages while eliminating their disadvantages [15].

The nonlinear optimal control law derived from the numerical methods cannot correct state errors introduced during the control period. The second objective of this work is to design a neighboring optimal guidance scheme which is able to take the perturbed trajectory to the desired manifold by tracking a given optimal trajectory in real time. This off-line optimal trajectory planning and on-line near-optimal guidance strategy may shed new light on the solution of general spacecraft attitude maneuvers.

The following dissertation is divided into six subsequent chapters. In Chapter 2, several commonly-used direct and indirect iteration methods and their applications are illustrated and discussed through an optimal control example. Chapter 3 includes the derivations of the dynamical model that governs the attitude motions of rigid spacecraft with multiple internal and external torque mechanisms. The optimal multi-axis attitude control of rigid spacecraft with external torque mechanisms aligned in three principal body axes is discussed in Chapter 4. Several strategies for the construction of starting trajectories associated with the method of particular solutions are compared through the examples of spacecraft reorientation. The coupling of a first-order gradient method with the method of particular solutions is also presented and examples which demonstrate the effectiveness of the approach are given. In Chapter 5, the problem of optimal attitude control of spacecraft with internal reaction wheels is also treated by the method of particular solutions alone and by the hybrid approach. A real-time near-optimal guidance scheme for formulating a neighboring optimal trajectory along a given optimal trajectory is presented in Chapter 6 and a numerical example is provided. Finally, in Chapter 7, the results of this research are summarized and examined, and topics for further research are suggested.

CHAPTER 2

COMPUTING METHODS FOR SOLVING TWO-POINT BOUNDARY-VALUE PROBLEMS

Using any iterative solution technique for solving a NTPBVP associated with an optimal control problem, one must formulate an initial nominal solution which may satisfy a certain combination of (1) the constraint differential equations, (2) the optimality conditions, and (3) the initial and final boundary conditions, or none of the above, depending upon the characteristics of the technique. Then through iterative procedures, an optimal solution which satisfies the boundary conditions and all the constraint conditions may be found. The solution reliability depends not only on the numerical methods employed but also on the formulation of a good starting solution based upon knowledge of the physical system. In general, all the iteration methods reported in the area of solving optimal control problems can be categorized as either direct or indirect [16,17].

Several commonly-used iteration methods are reviewed and discussed in this chapter. These methods fall into groups of similar fundamental character. Together, they span most the spectrum of the iteration methods. The formulations, presented in general terms, are directly applicable to this research. An example of an optimal control problem consisting of two coupled nonlinear first-order ordinary differential equations is provided to demonstrate the characteristics of these methods.

2.1 Statement of the Optimal Control Problem

A general optimal control problem of a dynamical system can be formulated in vector form as follows. For a given set of n-order nonlinear state equations

$$\dot{\underline{x}}(t) = f(\underline{x}(t), \underline{u}(t), t) \qquad 0 < t < t_f \tag{2.1}$$

with the specified initial and final boundary conditions

$$\underline{x}(0) = \underline{a}\ , \quad \underline{x}(t_f) = \underline{b}\ , \tag{2.2}$$

the optimal control task is to find an optimal trajectory which transfers the system from the initial states to the final states while minimizing the cost functional

$$J = \int_0^{t_f} F(\underline{x}(t), \underline{u}(t), t)dt + \psi(\underline{x}(t_f)) \tag{2.3}$$

where $\underline{x}$ and $\underline{u}$ are the state vector of order n and the control vector of order m, respectively. The vectors $\underline{a}$ and $\underline{b}$ are constant and of order n, and the final time t_f is fixed. The Hamiltonian of the system is defined as

$$H = F(\underline{x}(t), \underline{u}(t), t) + \underline{\lambda}^T f(\underline{x}(t), \underline{u}(t), t) \tag{2.4}$$

where $\underline{\lambda}$ is the Lagrange multiplier or costate vector of order n. The first-order necessary conditions of optimality are [18]

$$\dot{\underline{\lambda}}(t) = -\frac{\partial H}{\partial \underline{x}} \tag{2.5}$$

$$\frac{\partial H}{\partial \underline{u}} = 0 \tag{2.6}$$

Together, Eqs. (2.1), (2.5), and the boundary conditions (2.2) form a NTPBVP. Any solution to this NTPBVP also has to satisfy the optimality condition (2.6) in order to be a solution candidate for the optimal control problem. The boundary conditions are split between initial and final states, but no boundary condition is specified in the

costates. Thus any forward or backward numerical integration is impossible until the missing costate conditions are determined.

2.2 Direct Methods

In the case of direct methods, iterative gradient techniques are applied in the function space in the search for extremals of the cost functional. A sequence of descent directions is made and the control is successively modified until a minimum value of the cost functional is achieved.

First-Order Gradient Method (FOGM)

A typical method in the category of direct methods is the first-order gradient method. Varied derivations of the first-order gradient method can be found in different literatures [16,19]; however, the results are fundamentally the same. The formulation presented below is modified from Merriam [20]. A penalty term is added to the cost functional such that the fixed final boundary conditions are treated as free boundaries, and the final time is fixed. The cost functional in Eq. (2.3) is rewritten as follows:

$$J = \int_0^{t_f} [H(\underline{x}(t), \underline{u}(t), \underline{\lambda}(t), t) - \underline{\lambda}^T \dot{\underline{x}}]dt + \frac{1}{2} (\underline{x}(t_f) - \underline{b})^T M(\underline{x}(t_f) - \underline{b})|_{t=t_f} \qquad (2.7)$$

where $\underline{b}$ is the desired final boundary condition and the penalty matrix M is diagonal with large positive elements. The iterative final boundary $\underline{x}(t_f)$ can be forced toward $\underline{b}$ by increasing the values of the diagonal elements of M so long as no numerical singularity occurs. The functions then can be expanded by Taylor series about the

previous iteration, provided the changes in system variables are small between two consecutive iterations. Let

$$H^{i+1} \cong H^i + \frac{\partial H^i}{\partial \underline{x}^i}\delta\underline{x} + \frac{\partial H^i}{\partial \underline{u}^i}\delta\underline{u} + \frac{\partial H^i}{\partial \underline{\lambda}^i}\delta\underline{\lambda}$$
$$\delta\underline{\theta} = \underline{\theta}^{i+1} - \underline{\theta}^i$$

where $\underline{\theta}$ can be $\underline{x}$, $\underline{u}$, $\underline{\lambda}$, or $\dot{\underline{x}}$. Accordingly, the $(i+1)^{th}$ iteration of the cost functional (2.7) can be expressed by neglecting second- and higher-order terms as

$$J^{i+1} \cong J^i + \int_0^{t_f}\left[\frac{\partial H^i}{\partial \underline{x}^i}\delta\underline{x} + \frac{\partial H^i}{\partial \underline{u}^i}\delta\underline{u} + \frac{\partial H^i}{\partial \underline{\lambda}^i}\delta\underline{\lambda} - \delta\underline{\lambda}^T\dot{\underline{x}}^i - (\underline{\lambda}^i)^T\delta\dot{\underline{x}}\right]dt + \delta\underline{x}^T M(\underline{x}^i - \underline{b})\Big|_{t=t_f} \tag{2.8}$$

Substituting the state and costate equations into Eq. (2.8) yields

$$J^{i+1} \cong J^i + \int_0^{t_f}\frac{\partial H^i}{\partial \underline{u}^i}\delta\underline{u}\,dt - (\underline{\lambda}^i)^T\delta\underline{x}\Big|_0^{t_f} + \delta\underline{x}^T M(\underline{x}^i - \underline{b})\Big|_{t=t_f} \tag{2.9}$$

Let the new boundary conditions of the problem be

$$\underline{x}(0) = \underline{a} \quad , \quad \underline{\lambda}(t_f) = M(\underline{x}(t_f) - \underline{b})$$

and Eq. (2.9) is thus reduced to

$$J^{i+1} - J^i \cong \int_0^{t_f}\frac{\partial H^i}{\partial \underline{u}^i}\delta\underline{u}\,dt \tag{2.10}$$

To establish a descent property for the iteration to reach a minimum, we choose

$$\delta \underline{u} = -\alpha \frac{\partial H^i}{\partial \underline{u}^i} \qquad 0 < \alpha \leq 1 \tag{2.11}$$

and update the (i + 1)th control history by

$$\underline{u}^{i+1} = \underline{u}^i - \alpha \frac{\partial H^i}{\partial \underline{u}^i} \tag{2.12}$$

The method is largely independent of the initial guess. It has the property of fast convergence in the first few iterations and slow final convergence. However, if the undetermined step size α and the constants in the penalty matrix are not properly chosen, the trajectory may oscillate from one iteration to the next without actually reducing the cost functional [21].

Second-Order Gradient Method (SOGM)

A natural extension of the FOGM is the inclusion of the second-order variation terms in the expansion of the cost functional which is to be minimized. Several versions of the second-order gradient method and their modifications are discussed in [22]. The advantages of the second-order gradient method over the FOGM are the fast convergence rate near an optimal solution and, as side products, the implicit checks of the convexity, normality, and conjugate-point conditions, which are the sufficient conditions for the trajectory to be a local minimum [16,17]. Also, the step size α may be automatically determined and the penalty function can be dropped with the trajectory satisfying the final boundary conditions exactly in the final stage of iterations [23]. The disadvantages are the excessive programming effort and memory requirement, difficulty in the inversion of the Hessian matrix, convergence only near an optimal solution, and the convexity condition, which requires that the nominal

solution has the condition $\partial^2 H/\partial \underline{u}^2 > 0$ at all time during the iteration process. An initial nominal solution close to the optimal solution is required to insure successful convergence of the method.

Conjugate Gradient Method (CGM)

The conjugate gradient method is a modified algorithm of the first-order gradient method which attempts to combine the advantages of both first-order and second-order methods while at the same time eliminating some of their disadvantages. Many different versions of this method have been reported [24], and they all possess the same two processes. One is to generate a sequence of directions which are orthogonal or conjugate to each other with respect to $\partial^2 J/\partial \underline{u}^2$. The other is to perform a sequence of one-dimensional searches along each conjugate direction for a minimum, which subsequently becomes the new starting search point for the next conjugate direction.

An algorithm based on the work of Fletcher and Reeves [25] is introduced in the following. No evaluation of the second-order term is required. Given an initial estimated control history $\underline{u}^0(t)$, the step sizes and directions of reducing the cost functional can be determined by

$$
\begin{aligned}
&\underline{g}_0 = -\frac{\partial H^0}{\partial \underline{u}^0} \quad \text{and} \quad \underline{d}_0 = \underline{g}_0 \\
&\underline{u}^{l+1} = \underline{u}^l + \alpha_l \underline{d}_l \\
&\alpha_l = \alpha \qquad \text{which minimizes } H(u^l + \alpha \underline{d}_l) \\
&\underline{d}_{l+1} = -\underline{g}_l + \beta_l \underline{d}_l \\
&\beta_l = \frac{\underline{g}_{l+1}^T \underline{g}_{l+1}}{\underline{g}_l^T \underline{g}_l}
\end{aligned}
\tag{2.13}
$$

where H^0 is the system Hamiltonian associated with the starting solution, $\underline{g}_i$ is the gradient of H^i with respect to $\underline{u}^i$, and i= 1, 2, 3, ... is the iteration number. Though the step sizes and descent directions can be determined automatically in the iteration procedures, difficulties still remain in satisfying the specified final boundary conditions completely and in searching for a minimum point along a conjugate direction accurately. The first difficulty is due to the fact that the final boundary conditions must be treated by a penalty function. The latter is because the method is quite sensitive to the accuracy of the minimum in each direction, which is necessary for each search direction to be conjugately orthogonal. A good line search routine is essential to the success of the method. Generally, the CGM is not preferable unless the problem at hand has more than hundreds of variables [21].

2.3 Indirect Methods

With indirect methods, the state and costate differential equations are coupled by substituting the costates for the control variables through the use of necessary conditions of optimality. The constraint differential equations are then linearized about a proposed nominal solution, and the specified boundary values are utilized to yield a better estimate of the missing boundary values and a new nominal solution.

The Method of Particular Solutions (MPS)

The MPS reported by Miele and Iyer [26] is a similar version to the general Newton-Raphson method [23]. To illustrate the basic idea of this method, the state-costate equations are rewritten as

$$\dot{\underline{y}}(t) = \underline{g}(\underline{y}(t)) , \qquad 0 \leq t \leq t_f \tag{2.14}$$

with split boundary conditions

$$\begin{aligned} \underline{y}(0)_i &= a_i \quad (i = 1, 2, \ldots, p) \\ [C]\underline{y}(t_f) &= \underline{b} \end{aligned} \tag{2.15}$$

where $y = (\underline{x}, \underline{\lambda})^T$ is a 2n x 1 vector, [C] is a known q x 2n constant matrix, $\underline{b}$ is a given q x 1 vector, and p + q = 2n. A nominal solution $\tilde{\underline{y}}(t)$ is chosen and may satisfy the initial boundary conditions only. Let $\underline{y}(t) = \tilde{\underline{y}}(t) + \delta\underline{y}(t)$, where $\underline{y}(t)$ is a solution satisfying Eq. (2.14) and boundary conditions (2.15) to the first order. Linearizing Eq. (2.14) gives

$$\dot{\underline{y}} = g(\tilde{\underline{y}}) + \frac{\partial g(\tilde{\underline{y}})}{\partial \underline{y}} \delta\underline{y} + \ldots \qquad 0 \le t \le t_f \tag{2.16}$$

The unknown $\delta\underline{y}$ term in Eq. (2.16) represents the first-order deviation between a nominal solution and an optimal solution. We may also substitute $\delta\underline{y} = \underline{y} - \tilde{\underline{y}}$ into Eq. (2.16) and obtain

$$\dot{\underline{y}} = g(\tilde{\underline{y}}) + \frac{\partial g(\tilde{\underline{y}})}{\partial \underline{y}} (\underline{y} - \tilde{\underline{y}}) + \ldots \qquad 0 \le t \le t_f \tag{2.17}$$

Ideally, the nominal solution is close to the desired optimal solution, in which case the first-order deviation is truly small and the linearization of the equations is valid to the first order. In practice, however, the initial nominal solution may not be close to an optimal solution. A scaling factor ε, where $0 < \varepsilon \le 1$, is introduced to control the deviation, $\underline{y} - \tilde{\underline{y}}$, to prevent $\underline{y}$ from changing too rapidly in a given iteration. To formulate the optimal solution, let

$$\underline{y}^j = \underline{y}^j(t) \qquad j = 1, 2, \ldots, q+1$$

denote q + 1 particular solutions obtained by forward numerical solution of Eq. (2.17) with the following q + 1 sets of initial conditions:

$$y_i^j(0) = a_i, \qquad i = 1, 2, ..., p, \quad j = 1, 2, ..., q+1$$
$$y_{p+k}^j(0) = \delta_{jk}, \quad k = 1, 2, ..., q, \quad j = 1, 2, ..., q+1$$

where δ_{jk} is the Kronecker delta. Because the differential equation (2.17) is linear, we can obtain another nominal solution by superimposing the q + 1 particular solutions which satisfy Eq. (2.17),

$$\underline{y}(t) = \sum_{j=1}^{n+1} k_j \underline{y}^j(t) \tag{2.18}$$

where the q + 1 constants k_j can be determined by imposing the boundary conditions (2.15) and solving the following q + 1 linear algebraic equations

$$\sum_{j=1}^{q+1} k_j = 1 \qquad \text{and} \qquad [C] \sum_{j=1}^{q+1} k_j \underline{y}^j(t_f) = \underline{b} \tag{2.19}$$

Then the new nominal solution is used to formulate another set of particular solutions, and an optimal solution may finally be constructed.

The MPS has been shown to be attractive in solving optimal control problems with many degrees of freedom. It has a quadratic convergence rate [22] near the optimal solution. However, like any other indirect method, the inherent computational difficulty with the MPS is to provide an initially near-optimal solution. This unique requirement is a direct result of the characteristics of the mathematical model. The coupled state and costate first-order variational equations are actually adjoint

differential equations linearized about an extremal solution. Either set of equations has an exponentially decreasing behavior, and the other set possesses an exponentially increasing behavior. This unstable phenomenon often causes direct integration of the system equations to fail and makes the method very sensitive to the initial guess. Moreover, small errors from guessing the unspecified initial costates may produce blow-up errors in the state or costate final boundaries [27].

Because of this starting difficulty, a robust and practical modification of this iterative algorithm must include a front end processor which can generate a near-optimal solution in a few iterations. A feasible approach is to use a gradient method like the FOGM, which has the characteristics of fast inital convergence and also demonstrates low sensitivity toward initial guesses. A combination of the two may create a strong and fast-convergence numerical method in solving the NTPBVP of optimal control maneuvers [14,28].

Several indirect methods which have similar formulation and convergence rate are summarized in [11,14]. The MPS will be used in this research, and the results gained may be also applicable to other indirect methods.

2.4 Numerical Example

The following example is chosen to illustrate and compare the methods discussed in the previous sections. We seek to minimize the cost functional

$$J = \frac{1}{2}\int_0^1 u^2(t)dt$$

subject to the constraint equations

$$\dot{x}_1 = -x_1x_2 + u$$
$$\dot{x}_2 = \frac{1}{2}(x_1^2 - x_2^2)$$

and the boundary conditions

$$x_1(0) = 1 \qquad x_1(1) = -0.7$$
$$x_2(0) = -0.3 \qquad x_2(1) = 1$$

From Eqs. (2.5) and (2.6), the costate equations are

$$\dot{\lambda}_1 = x_2\lambda_1 - x_1\lambda_2$$
$$\dot{\lambda}_2 = x_1\lambda_1 + x_2\lambda_2$$

and the optimality condition for a solution is

$$u + \lambda_1 = 0$$

Using Eq (2.17) to linearize the state-costate equations yield

$$\dot{x}_1 = -(x_1x_{2n} + x_{1n}x_2 - x_{1n}x_{2n}) + u$$
$$\dot{x}_2 = x_1x_{1n} + x_2x_{2n} - \frac{1}{2}(x_{1n}^2 - x_{2n}^2)$$
$$\dot{\lambda}_1 = x_2\lambda_{1n} - x_{2n}\lambda_1 - x_1\lambda_{2n} - x_{1n}\lambda_2 - (x_{2n}\lambda_{1n} - x_{2n}\lambda_{1n})$$
$$\dot{\lambda}_2 = x_1\lambda_{1n} + x_{1n}\lambda_1 + x_2\lambda_{2n} + x_{2n}\lambda_2 - (x_{1n}\lambda_{1n} + x_{2n}\lambda_{2n})$$

where x_i and λ_i are the solutions, and x_{in} and λ_{in} are the nominal solutions, as previously defined in Section 2.3. Four methods, FOGM, FOGM with line search, CGM, and MPS were applied to this example. The same time step, 0.01, and starting nominal solution, linear between the initial and final states, were used for all the methods. For FOGM, the control step α is fixed at 8×10^{-10} and the penalty matrix diagonal elements at 5×10^{9}. Also, to compare FOGM with line search routine and CGM, the quadratic function was used in both methods, the initial control step size is set at 0.002, and the diagonal elements of the penalty matrix are given the value of 5000. By assuming that the cost functional can be approximated by a quadratic function near the minimum along a descent direction, we define

$$J(u_j) = u_j^2 + bu_j + c \tag{2.20}$$

where $J(u_j)$ is the cost functional, u_j is the control variable, and j = i-1, i, i+1 with $J(u_i)$ being the smallest among the three consecutive values. The approximate minimum along a descent direction may be determined by solving the constants b and c in Eq. (2.20). However, if the approximation is not close to the minimum, as it can be perceived in the example, the method will not converge. The iteration results are compared in Table 2.1, and the optimal trajectory of the example is shown in Fig 2.1. The iteration process was terminated for the FOGM with line search and the CGM at 58 and 20 iterations, respectively, because of failure of the algorithms to progress toward the optimal solution. The value of $\lambda_i(t)$ is about one order higher than the value of $x_i(t)$ so that even if the trajectory is uncomplicated the iteration process does not converge easily.

2.5 Concluding Remarks

Different types of gradient methods have been discussed in this chapter. The FOGM has shown several advantages over other gradient methods, namely, the formulations are straightforward and simple and the convergence requirements are not contingent upon a good initial estimate as a starting condition. Furthermore, the technique assures that the cost functional to be minimized decreases after each iteration. The major disadvantage of this type of method, as discussed previously, is its slow convergence as the optimal trajectory is approached.

In contrast, the MPS, like the other indirect methods, is sensitive to the initial estimate but converges quadratically near an optimal solution. The FOGM and CGM using a linear search routine may not be effective in formulating an optimal trajectory.

Table 2.1 Comparison of Methods for Example 2.1

	No. of Iterations	Iterated State $x_1(1)$	Iterated State $x_2(1)$
FOGM with Line Search	58	-0.59261	0.81634
CGM	20	-0.97567	-0.13831
FOGM	21	-0.70001	1.00000
MPS	9	-0.70000	1.00000

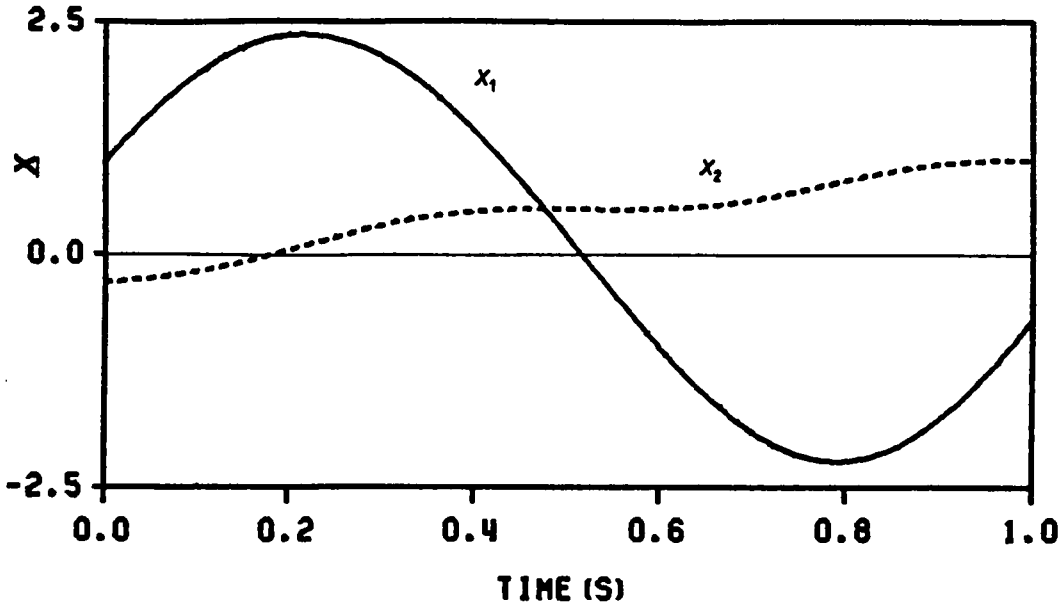

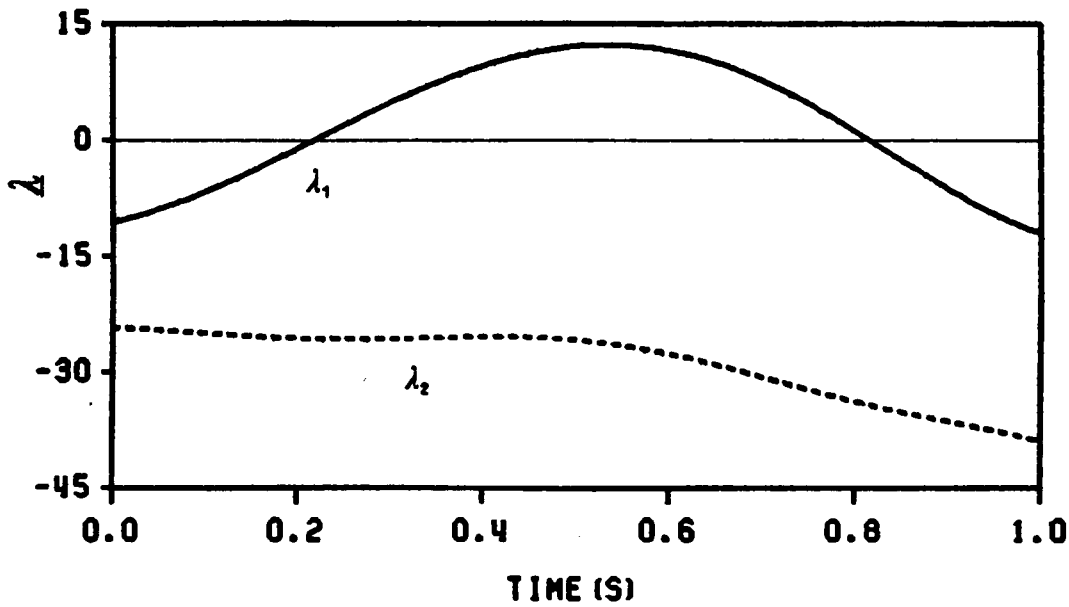

Figure 2.1 Optimal Trajectory for Example 2.1

Even with a good line search routine, the computing time spent on searching for minima along the sequence of descent directions can be very costly. From the numerical results given in Table 2.1, the FOGM, which has a linear convergence speed [29], combined with the MPS can be a fast and reliable iteration algorithm in solving a general nonlinear two-point boundary-value problem.

Detailed discussions of variations of the discussed methods can be found in the literature [30,31] and are not repeated here. Other methods, such as Chebyshev polynomials, finite difference method, and dynamic programming, have limited applications in this case [11,22] either because of their dimensionality problems or natural limitation to the high-order nonlinear problems and will not be discussed further.

CHAPTER 3

ATTITUDE MOTIONS OF RIGID SPACECRAFT

Before discussing the problem of spacecraft attitude dynamics and control, we need to determine how to specify the orientation of the spacecraft during the maneuver. Direction cosines, Euler angles, and Euler parameters are commonly used for the kinematics of rotation. For large-angle rotations, three parameters are required to specify the orientation of a rigid body in inertial space; however, in order to avoid numerical difficulties, at least four variables are needed to specify the angular motion. Euler parameters, which are associated with Euler's Theorem and contain four variables (once-redundant), have been recognized as the most useful ones for spacecraft large-angle rotational motion. Unlike Euler angles or direction cosines which suffer from nonlinear trigonometric functions and singularity problems, the time rates of change of Euler parameters are linear with respect to angular velocity components and are computationally free from singularity problems [32,33,34]. The Euler-parameter representation of the orientation will be used throughout this research.

3.1 Kinematics of Rotational Motions

As stated in Euler's Principal Rotational Theorem, one can describe a general rigid-body rotation from any initial orientation to an arbitrary final orientation by a single rotation of the body through a principal angle Φ about a principal axis l fixed both in the body and in inertial space. Let the Euler parameters be defined as [32]

$$\beta_0 = \cos\frac{\Phi}{2}\ ,\quad \beta_1 = l_1 \sin\frac{\Phi}{2}\ ,\quad \beta_2 = l_2 \sin\frac{\Phi}{2}\ ,\quad \beta_3 = l_3 \sin\frac{\Phi}{2} \tag{3.1}$$

where the l_i are direction cosines of the principal axis of rotation. Note that the β_j satisfy the constraint

$$\sum_{j=0}^{3} \beta_j^2 = 1 \tag{3.2}$$

If the history of the body angular velocity is known, then the rate of change of the β_j are given by

$$\dot{\underline{\beta}} = [G(\omega)]\underline{\beta} \tag{3.3}$$

where

$$\underline{\beta} = (\beta_0, \beta_1, \beta_2, \beta_3)^T, \quad [G(\omega)] = \frac{1}{2}\begin{bmatrix} 0 & -\omega_1 & -\omega_2 & -\omega_3 \\ \omega_1 & 0 & \omega_3 & -\omega_2 \\ \omega_2 & -\omega_3 & 0 & \omega_1 \\ \omega_3 & \omega_2 & -\omega_1 & 0 \end{bmatrix}$$

and the ω_i are principal body-axis components of angular velocity. As mentioned earlier, the differential equations (3.3) are linear and involve no trigonometric functions. Although the time-dependent coefficients in Eq. (3.3) preclude analytical solutions, the constraint Eq. (3.2) can be used to check numerical accuracy when problems are solved by computer.

3.2 Rigid Spacecraft Attitude Dynamics with Reaction Wheels

Internal reaction wheels and external expansion jets are two commonly used torque-generating mechanisms in spacecraft attitude control. The equations of atti-

tude motion of a rigid spacecraft using these two mechanisms are formulated in this section. The angular momentum with respect to the system center of mass C of the N-wheel spacecraft of Fig. 3.1 can be expressed as follows [35]:

$$\underline{H}_C = \underline{H}^{B/C} + \sum_{i=1}^{n} \underline{H}^{C_i/C} \tag{3.4}$$

where $\underline{H}_c$ is the total angular momentum of the system,

$$\underline{H}^{B/C} = \int_{Body} \underline{\rho} \times \dot{\underline{\rho}}\, dm \tag{3.5}$$

is the body angular momentum vector of the spacecraft with respect to C excluding the wheels, and $\underline{H}^{C_i/C}$ is the angular momentum vector of the i^{th} wheel referenced to C. For a rigid spacecraft,

$$\dot{\underline{\rho}} = {}^{N}\underline{\omega}^{B} \times \underline{\rho},$$

which leads to

$$\underline{H}^{B/C} = \int_{Body} \underline{\rho} \times ({}^{N}\underline{\omega}^{B} \times \underline{\rho}) dm \qquad \text{or} \qquad \underline{H}^{B/C} = [I]^{Body}\{{}^{N}\omega^{B}\}$$

where ${}^{N}\underline{\omega}^{B}$ is the angular velocity of the spacecraft, $\underline{\rho}$ is the position vector of dm relative to C,

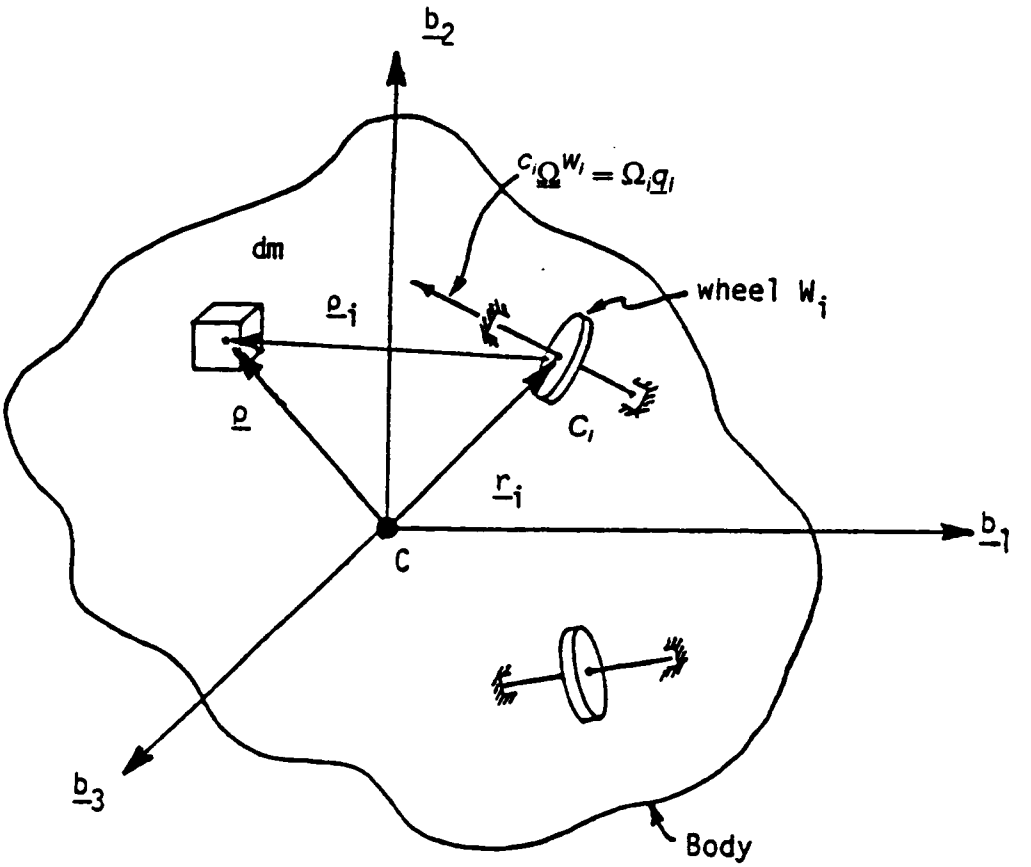

Figure 3.1 Rigid Spacecraft with N Reaction Wheels

$$[I]^{Body} = \begin{bmatrix} I_{11} & I_{12} & I_{13} \\ I_{21} & I_{22} & I_{23} \\ I_{31} & I_{32} & I_{33} \end{bmatrix}^{Body}$$

is the body moment of inertia matrix referenced to C, and $\{^N\omega^B\} = \{\omega_1, \omega_2, \omega_3\}$ are the components of spacecraft angular velocity. The angular momentum of the i^{th} wheel W_i can be expressed as

$$H^{C_i/C} = \int_{W_i} (\underline{\rho}_i + \underline{r}_i) \times (\dot{\underline{\rho}}_i + \dot{\underline{r}}_i)\, dm \tag{3.6}$$

where $\underline{\rho}_i$ is the position vector of dm in terms of coordinates $\underline{g}_i$ fixed on the i^{th} wheel, and $\underline{r}_i$ is the position vector of the center of mass C_i of the i^{th} wheel relative to C. Expanding Eq. (3.6) gives

$$H^{C_i/C} = (\underline{r}_i \times \dot{\underline{r}}_i)\int_{W_i} dm + \underline{r}_i \times \int_{W_i} \dot{\underline{\rho}}_i dm - \dot{\underline{r}}_i \times \int_{W_i} \underline{\rho}_i dm + \int_{W_i} (\underline{\rho}_i \times \dot{\underline{\rho}}_i) dm$$

Note that

$$\int_{W_i} \underline{\rho}_i dm = 0\,, \qquad \int_{W_i} \dot{\underline{\rho}}_i dm = 0 \quad \text{and} \quad \int_{W_i} dm = M_{W_i}$$

where M_{W_i} is the total mass of the i^{th} wheel. Let $\int_{W_i} (\underline{\rho}_i \times \dot{\underline{\rho}}_i) dm$ be expressed in terms of body fixed coordinates $\underline{b}$ and rewrite the sum of the wheel angular momenta with respect to C as

$$\sum_{i=1}^{n} \underline{H}^{C_i/C} = \sum_{i=1}^{n} M_{W_i}(\underline{r}_i \times \dot{\underline{r}}_i) + \sum_{i=1}^{n} [I_{W_i}]^{C_i/C}\left[\{{}^N\omega^B\} + \{{}^N\Omega^{W_i}\}\right] \tag{3.7}$$

where

$$[I_{W_i}]^{C_i/C} = \begin{bmatrix} I_{11} & I_{12} & I_{13} \\ I_{21} & I_{22} & I_{23} \\ I_{31} & I_{32} & I_{33} \end{bmatrix}^{C_i/C}$$

is the moment of inertia of i^{th} wheel referenced to C in $\underline{b}$, and $\{{}^N\Omega^{W_i}\}$ is the angular velocity of i^{th} wheel in terms of $\underline{b}$. A transformation also exists that

$$\{{}^N\Omega^{W_i}\} = [T]^{C_i/C}\{{}^{C_i}\Omega^{W_i}\}$$

where $[T]^{C_i/C}$ is the 3 x 3 transformation matrix from coordinates $\underline{q}_i$ fixed on the i^{th} wheel to body-fixed coordinates $\underline{b}$, and $\{{}^{C_i}\Omega^{W_i}\}$ is the angular velocity of i^{th} wheel in $\underline{q}$. Let

$$\underline{r}_i = x_i\underline{b}_1 + y_i\underline{b}_2 + z_i\underline{b}_3$$

and

$$\dot{\underline{r}}_i = {}^N\underline{\omega}^B \times \underline{r}_i$$

The total angular momentum of the N wheels (3.7) can be written as

$$\sum_{i=1}^{n} H^{C_i/C} = \sum_{i=1}^{n} \{[I_{W_i}]^{C_i/C} + [K_i]\}\{{}^{N}\omega^{B}\} + \sum_{i=1}^{n} [I_{W_i}]^{C_i/C}[T]^{C_i/C}\{{}^{C_i}\Omega^{W_i}\} \tag{3.8}$$

where

$$[K_i] = M_{W_i}\begin{bmatrix} (y_i^2 + z_i^2) & -x_i y_i & -x_i z_i \\ -x_i y_i & (x_i^2 + z_i^2) & -y_i z_i \\ -x_i z_i & -y_i z_i & (x_i^2 + y_i^2) \end{bmatrix}$$

Substituting Eq. (3.6) and (3.8) into (3.4) and rearranging the equation, we can then express the total angular momentum Eq. (3.4) as

$$H_C = [I]\{{}^{N}\omega^{B}\} + [A]\{\Omega\} \tag{3.9}$$

where

$$[I] = [I]^{Body} + \sum_{i=1}^{n} \{[I_{W_i}]^{C_i/C} + [K_i]\} \ ,$$

$$[A] = \left[[I_{W_1}]^{C_1/C}[T]^{C_1/C} \,|\, [I_{W_2}]^{C_2/C}[T]^{C_2/C} \,|\, \ldots \,|\, [I_{W_n}]^{C_n/C}[T]^{C_n/C} \right]$$

and

$$\{\Omega\} = \{{}^{C_1}\Omega^{W_1}\ {}^{C_2}\Omega^{W_2} \ldots {}^{C_n}\Omega^{W_n}\}^{T}$$

is a 3n x 1 vector of reaction wheel angular speeds. From the Transport Theorem, the time rate of change of the total momentum is

$$\underline{U}_C = \frac{d\underline{H}_C}{dt}\Big|_b + \underline{\omega} \times \underline{H}_C \tag{3.10}$$

where $\underline{U}_c$ is the vector of external torque. Expanding Eq. (3.10) yields

$$\underline{U}_C = [I]\{\dot{\omega}\} + [A]\{\dot{\Omega}\} + [\tilde{\omega}][I]\{\omega\} + [\tilde{\omega}][A]\{\Omega\} \tag{3.11}$$

where

$$[\tilde{\omega}] = \begin{bmatrix} 0 & -\omega_3 & \omega_2 \\ \omega_3 & 0 & -\omega_1 \\ -\omega_2 & \omega_1 & 0 \end{bmatrix}$$

Equations (3.3) and (3.11) represent the general attitude motion of a rigid spacecraft with internal reaction wheels and external torque mechanisms.

3.3 Concluding Remarks

The attitude equations of motion for a rigid spacecraft have been formulated. The control devices modeled include expansion jets and reaction wheels. The problem of any coupling to the motion of the center of mass is not considered in this work.

CHAPTER 4

RIGID SPACECRAFT GENERAL ATTITUDE MANEUVERS WITH OPTIMAL EXTERNAL CONTROL TORQUES

General nonlinear optimal control problems usually must be solved by numerical methods. The solution conditions for such problems are always cast in the form of boundary-value problems. The MPS discussed in Chapter 2 has shown some effectiveness in solving the NTPBVP [11] with many degrees of freedom, but it also requires a good initial estimate to achieve convergence. To increase the solution reliability of the MPS, four strategies designed to estimate the best possible starting or nominal solution are presented in this chapter. The starting solution may be made based upon knowledge of the physical system; however, a good estimate is quite improbable if the trajectory of the maneuver is nonlinear. To circumvent the difficulty, the hybrid approach of combining the FOGM with the MPS to utilize the best features of each is also presented. Two numerical examples of general optimal attitude maneuver problems for an externally-torqued rigid asymmetric spacecraft are chosen for comparing the methods.

4.1 Externally-Torqued Rigid Spacecraft Attitude Motions

The governing equations of attitude motion for a rigid, externally torqued spacecraft in body-fixed principal axes system are now formulated. Using Eq. (3.3) and (3.4) of Chapter 3 and eliminating the reaction-wheel terms in Eq. (3.11) give

$$\dot{\underline{\beta}} = [G(\omega)]\underline{\beta} \tag{4.1}$$

$$\dot{\omega}_1 = -J_1\omega_2\omega_3 + \frac{U_1}{I_1}$$
$$\dot{\omega}_2 = -J_2\omega_3\omega_1 + \frac{U_2}{I_2} \qquad (4.2)$$
$$\dot{\omega}_3 = -J_3\omega_1\omega_2 + \frac{U_3}{I_3}$$

The ω_i are principal body-axis components of angular velocity, the I_i are principal mass moments of inertia, the U_i are principal components of the external torque, the β_i are Euler parameters, and

$$J_1 = \frac{I_3 - I_2}{I_1}, \quad J_2 = \frac{I_1 - I_3}{I_2}, \quad J_3 = \frac{I_2 - I_1}{I_3}$$

Also, the β_i satisfy the constraint Eq. (3.2). Equations (4.1) and (4.2) represent the kinematics and kinetics of rotation for a rigid externally-torqued spacecraft.

4.2 Optimal Control Problems

Problem Formulations

To reorient a spacecraft from a known initial state to a specified final state at time t_f, the external torques U_i may be minimized in the sense of the commonly used cost functional

$$J = \frac{1}{2}\int_0^{t_f} [U_1^2(t) + U_2^2(t) + U_3^2(t)]\, dt$$

The Hamiltonian for the system is

$$H = \frac{1}{2}(U_1^2 + U_2^2 + U_3^2) + \underline{\lambda}^T \dot{\underline{\omega}} + \underline{\gamma}^T \dot{\underline{\beta}} \tag{4.3}$$

where $\underline{\lambda}$ and $\underline{\gamma}$ are the seven costates or Lagrange multipliers. The first-order necessary conditions of optimality for the optimal maneuver derived via Pontryagin's Principle are

$$\dot{\lambda}_I = -\frac{\partial H}{\partial \omega_I} \qquad (I = 1, 2, 3)$$

$$\dot{\gamma}_J = -\frac{\partial H}{\partial \beta_J} \qquad (J = 0, 1, 2, 3)$$

$$\frac{\partial H}{\partial U_I} = 0 \qquad (I = 1, 2, 3)$$

or

$$\begin{aligned}
\dot{\lambda}_1 &= J_2\lambda_2\omega_3 + J_3\lambda_3\omega_2 + \frac{1}{2}(\beta_1\gamma_0 - \beta_0\gamma_1 - \beta_3\gamma_2 + \beta_2\gamma_3) \\
\dot{\lambda}_2 &= J_1\lambda_1\omega_3 + J_3\lambda_3\omega_1 + \frac{1}{2}(\beta_2\gamma_0 + \beta_3\gamma_1 - \beta_0\gamma_2 + \beta_1\gamma_3) \\
\dot{\lambda}_3 &= J_1\lambda_1\omega_2 + J_2\lambda_2\omega_1 + \frac{1}{2}(\beta_3\gamma_0 - \beta_2\gamma_1 + \beta_1\gamma_2 - \beta_0\gamma_3)
\end{aligned} \tag{4.4}$$

$$\dot{\underline{\gamma}} = [G(\omega)]\underline{\gamma} \tag{4.5}$$

with the optimality conditions

$$U_I + \frac{\lambda_I}{I_I} = 0 \qquad (I = 1, 2, 3) \tag{4.6}$$

The state and costate equations are coupled through Eq. (4.6). Given the initial and final boundary conditions specified on ω_I and β_J and the final time t_f, Eqs. (4.1), (4.2), and (4.4)-(4.6) form a NTPBVP.

Conditions for Optimal $\underline{\gamma}(t)$

From the first-order necessary conditions of optimality, there may exist an infinite number of admissible $\underline{\gamma}(t)$, but they are not totally arbitrary. As shown in [36], $\underline{\gamma}(t)$ satisfying the skew-symmetric differential equation (4.5) must satisfy

$$\underline{\gamma}^T(t)\underline{\gamma}(t) = C_1^2 \qquad \text{and} \qquad \underline{\beta}^T(t)\underline{\gamma}(t) = C_2$$

where C_1 and C_2 are constants. Also $\underline{\gamma}(t) \neq \alpha\underline{\beta}(t)$, where α is a non-zero constant. If $\underline{\gamma}(t) = \alpha\underline{\beta}(t)$, the Hamiltonian of the system is independent of $\underline{\beta}(t)$ because $[G(\omega)]$ is skew-symmetric. Let an admissible $\underline{\gamma}$ be

$$\underline{\gamma} = \underline{\gamma}_{op} + \delta\underline{\gamma} \ , \tag{4.7}$$

where $\underline{\gamma}_{op}$ is an optimal solution and $\delta\underline{\gamma}$ is the deviation between an admissible solution and an optimal solution. For an autonomous system, the Hamiltonian is constant along an optimal trajectory [37], which implies

$$\delta\underline{\gamma}^T[G(\omega)]\underline{\beta} = 0$$

and it follows that

$$\delta\underline{\gamma} = \mu\underline{\beta} \tag{4.8}$$

with constant μ. Substituting $\delta\underline{\gamma}$ from Eq. (4.8) into Eq. (4.7) yields

$$\underline{\gamma} = \underline{\gamma}_{op} + \mu\underline{\beta} \ , \tag{4.9}$$

and the norm of $\underline{\gamma}$ can be found by premultiplying Eq. (4.9) with $\underline{\gamma}^T$

$$\underline{\gamma}^T\underline{\gamma} = \underline{\gamma}^T\underline{\gamma}_{op} + \mu\underline{\gamma}^T\underline{\beta} \qquad \text{or} \qquad C_1^2 = C_{op}^2 + 2\mu\underline{\gamma}_{op}^T\underline{\beta} + \mu^2$$

Thus C_1^2 is a function of μ and has a stationary value at the optimal norm C_{op}^2. The necessary condition for an optimal $\underline{\gamma}$ can be found by

$$\left.\frac{\partial C_1^2}{\partial \mu}\right|_{\mu=0} = 2\underline{\gamma}_{op}^T\underline{\beta} + 2\mu = 0 \qquad \text{or} \qquad \underline{\gamma}_{op}^T\underline{\beta} = 0 \tag{4.10}$$

4.3 Solution Procedures

A. Method of Particular Solutions (MPS)

Four strategies for formulating a good initial nominal solution for the MPS (as a stand-alone method) were investigated:

Strategy 1: Use straight lines between the initial and final state boundary conditions and constant costates (used in Reference [11]).

Strategy 2: Generate a torque-free solution by forward integration of the state differential equations using initial state boundary conditions, modify this solution by adding a function of time which ensures that the final boundary conditions are met as well, and use constant costates. The final boundary condition on β_3 is not imposed when finding the new nominal solution from the combination of trial solutions. Note that only six independent final boundary conditions may be imposed when a new nominal solution is formed by combining the trial solutions. Thus for Strategy 2, the nominal solutions (other than the initial nominal solution) do not satisfy the final boundary condition on β_3.

Strategy 3: Same as Strategy 2, but impose the final boundary condition on β_3 by adding to the trial solution combination for β_3 a function of time which ensures that the $\beta_3(t_f)$ condition is met.

Strateqy 4: Same as Strategy 3, but impose the constraint equation (4.10) initially (by appropriate choice of the initial y_j used in the trial solutions) and finally (by adding appropriate functions of time to the y_j trial solution combination). For the initial nominal solution, use the modified torque-free ω_j solutions in integrating Eq. (4.1) to form the β_j solutions, which are then modified to satisfy the final boundary conditions.

The nominal solutions in Strategy 2 through 4 are modified using the following equation:

$$x_N(t) = x_T(t) - \frac{t}{t_f}\{x_T(t) - [\frac{t}{t_f}(x(t_f) - x(0)) + x(0)]\} \tag{4.11}$$

where $x_N(t)$ is the starting or nominal trajectory, $x_T(t)$ is the torque-free or old nominal trajectory, x(0) is the specified initial boundary condition, and $x(t_f)$ is the given final boundary condition.

Because of the redundancy on β_j, there are only six independent state variables and thus we need only to formulate seven trial solutions in the MPS.

Hybrid Approach

The FOGM has low convergence sensitivity to the initial nominal solution and slow convergence rate near the optimal solution. In contrast, the MPS is sensitive to the initial guess but converges efficiently as the optimal solution is approached. Us-

ing the FOGM first to produce a good initial guess for the MPS to carry on further iterations, we are able to design an efficient algorithm with a high successful convergence rate. The hybrid procedure can be summarized as follows:

1. Use the initial angular velocity to generate torque-free trajectory.

2. Modify the trajectory to satisfy the final angular velocity.

3. Use the modified ω_i trajectories to generate nominal solutions for the U_i and β_i from Eqs. (4.1) and (4.2).

4. To generate the nominal solutions for the λ_i and γ_i, use the final boundary conditions from the final penalty term in FOGM and integrate Eqs. (4.4) and (4.5) backwards from $t = t_f$ to $t = 0$.

5. Determine new U_{i+1} from Eqs. (2.11) and (2.12).

6. Generate new state and costate trajectories by using new U_{i+1} .

7. If the switching criterion is satisfied, pass the solution over to MPS and use Strategy 4 to modified the combined trial solutions; if not, go to step 5.

4.4 Numerical Examples

Two examples of detumbling a spacecraft to pure spin on a single principal axis are given in Table 4.1. The spacecraft in Example 4.1 has lower initial and final angular velocities and undergoes shorter maneuver times than in Example 4.2. As can

Table 4.1 Two Case Conditions for Motion-to-Motion Maneuvers

Example 4.1

Principal Moments of Inertia (kg-m^2)		$I_1 = 100$	$I_2 = 115$	$I_3 = 136$
Initial Angular Velocities (rad/s)		$\omega_1 = 0.05$	$\omega_2 = -0.04$	$\omega_3 = 0.055$
Final Angular Velocities (rad/s)		$\omega_1 = -0.015$	$\omega_2 = 0$	$\omega_3 = 0$
Initial Euler Parameters	$\beta_0 = 1.$	$\beta_1 = 0$	$\beta_2 = 0$	$\beta_3 = 0$
Final Euler Parameters	$\beta_0 = 0.70711$	$\beta_1 = 0.35355$	$\beta_2 = 0.35355$	$\beta_3 = 0.5$

Final Maneuver Time: from 30 to 130 seconds

Example 4.2

Initial Angular Velocities (rad/s)	$\omega_1 = 0.1$	$\omega_2 = 0.08$	$\omega_3 = 0.2$
Final Angular Velocities (rad/s)	$\omega_1 = 0$	$\omega_2 = 0$	$\omega_3 = 0.12$

Final Maneuver Time: 150 seconds

Other system data are the same as in Example 4.1.

be expected, the maneuver case given in Example 4.2 is much more difficult to solve than the ones in Example 4.1.

The four starting and nominal solution strategies for the MPS in Section 4.3 were investigated using Example 4.1 for various maneuver times, with all other given conditions held constant. The results shown in Table 4.2 indicate a clear trend of improvement as the more sophisticated strategies are implemented. Comparison of Strategies 1 and 3 shows a doubling of the success rate from 43% to 86%. The one case which failed with Strategy 3 was successfully solved with Strategy 4. Note that the required number of iterations generally decreases as the improved strategies are incorporated.

The 130-second maneuver which failed with Strategy 4 was successfully solved by the hybrid method with nine iterations for the FOGM and four iterations for the MPS. The penalty matrix M in Eq. (2.7) was held constant with a weight of 1000 for the final ω_f and 100 for the final β_f and parameter α in Eq. (2.11) was also held constant at 0.001. The switching from the FOGM to the MPS was executed when the cost functional of present iteration was greater than that of previous iteration, and the trajectory from previous iteration was used as starting solution for the MPS. The time required for 1 MPS iteration is approximately equal to that required for 8 FOGM iterations.

The angular velocity, attitude, and optimal control torques associated with the 130-second maneuver are shown in Figs. 4.1 through 4.3, and the trajectories shown in each figure are (a) the initial nominal solution for the MPS, (b) the initial nominal solution for the hybrid method, (c) the trajectory at switching time in the hybrid method, and (d) the final optimal trajectory.

Table 4.2 Comparison of Strategies for Example 4.1

Strategy	Maneuver Time (s)	No. of Iterations	Convergence
1	30	-	No
	40	5	Yes
	50	11	Yes
	60	8	Yes
	70	-	No
	80	-	No
	100	-	No
2	30	5	Yes
	40	7	Yes
	50	6	Yes
	60	9	Yes
	70	-	No
3	30	5	Yes
	40	4	Yes
	50	5	Yes
	60	5	Yes
	70	6	Yes
	80	6	Yes
	100	-	No
4	30	3	Yes
	60	4	Yes
	100	5	Yes
	120	6	Yes
	130	-	No
Hybrid	130	9 FOGM/4 MPS	Yes

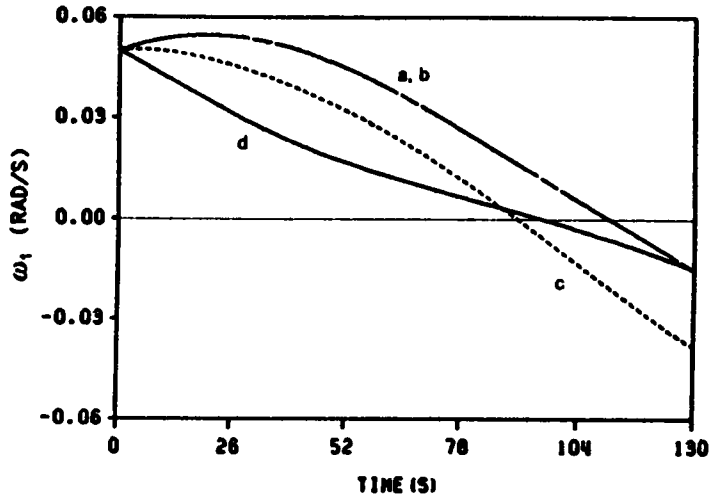

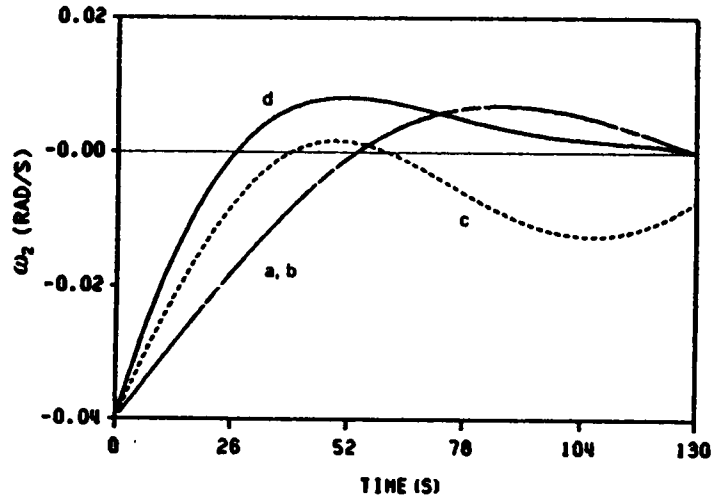

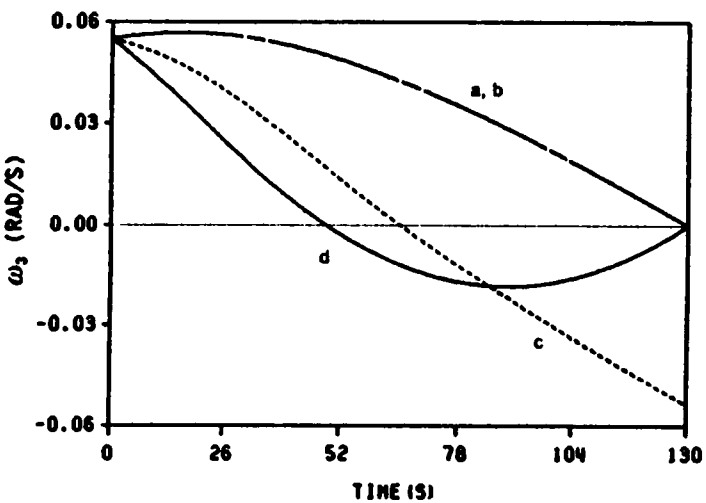

Figure 4.1 Comparison of 130-Second Angular Velocities for Example 4.1

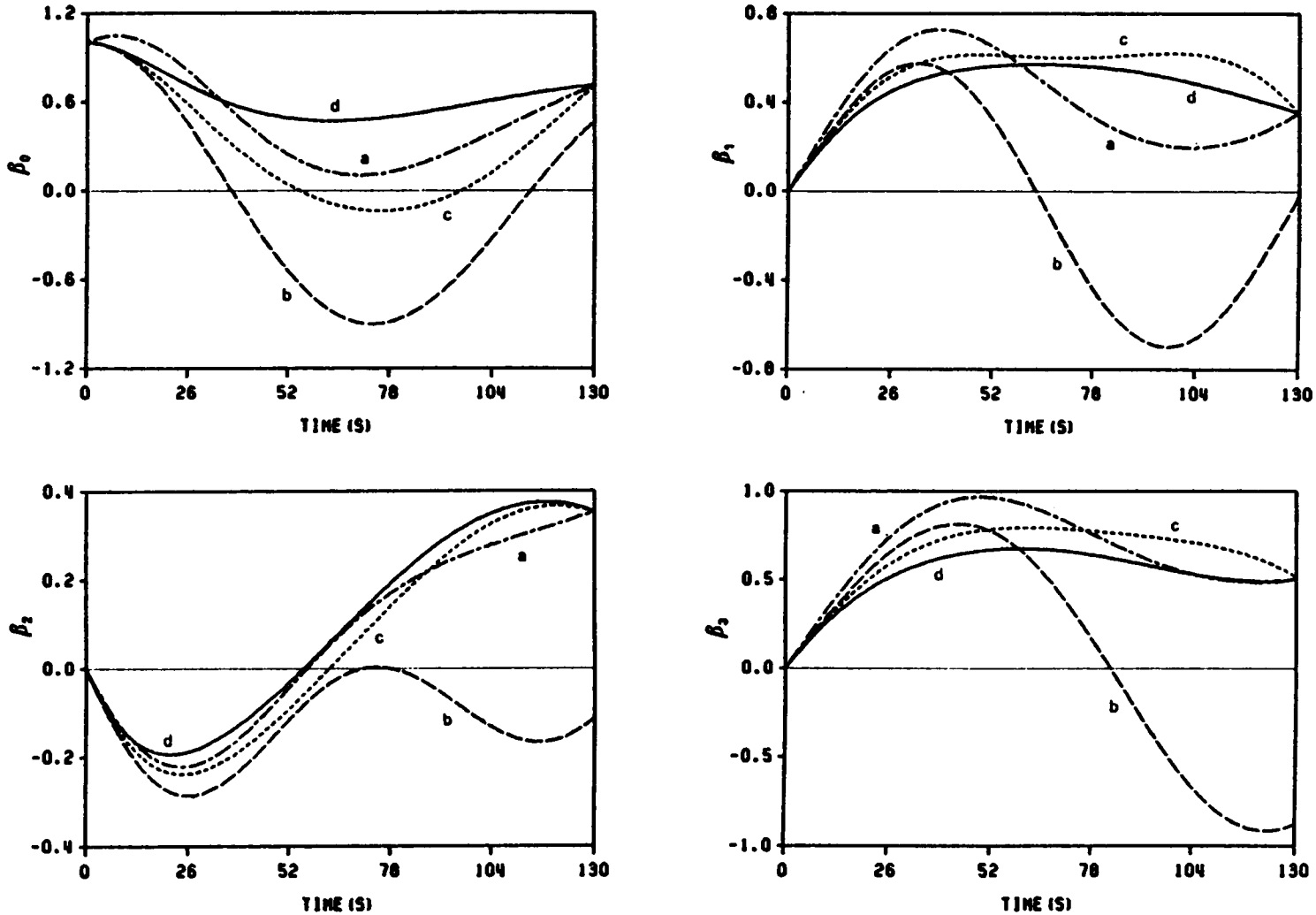

Figure 4.2 Comparison of 130-Second Euler Parameters for Example 4.1

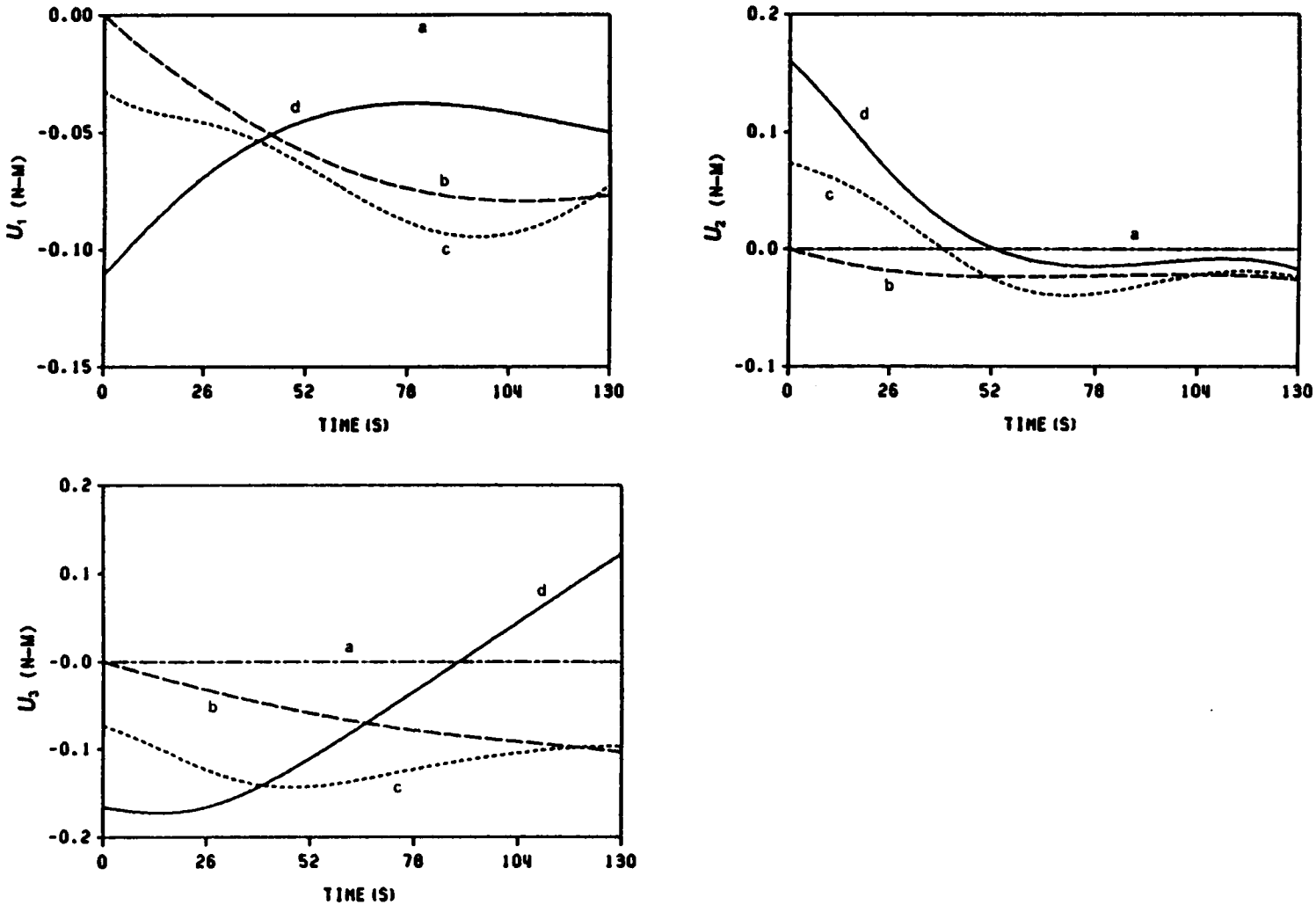

Figure 4.3 Comparison of 130-Second External Torques for Example 4.1

By studying these trajectories, we can find that, even with a poor initial estimate, the nominal trajectory (c) iterated from the FOGM has a closer shape and distance to the optimal trajectory (d) than the trajectory (a), the one generated by Strategy 4, has. Shown in Fig. 4.4 through 4.6 are the optimal trajectories for Example 4.2. This 150-second highly nonlinear trajectory with high angular velocity and many zero-crossing further demonstrates the effectiveness of the hybrid approach.

The same spacecraft model and designated orientations given in Example 4.1 were also used to test for the motion-to-rest, rest-to-motion, and rest-to-rest maneuver cases. Under the same initial angular velocity and maneuver times as in Example 4.1, the same trend of improvement as that shown in Table 4.2 has been found for the motion-to-rest case. The rest-to-motion and rest-to-rest maneuver cases turned out to be easier to solve than the previous two maneuver cases. For the same final angular velocity as given in Example 4.1, only six iterations were required to solve the 130-second rest-to-motion attitude maneuver when using the MPS with Strategy 4. The iterations required to solve the 180-second rest-to-rest case using the MPS with Strategy 1 and 4 were four and three, respectively.

4.5 Concluding Remarks

The convergence rate increases as the strategy for the MPS becomes more sophisticated. The reliability of the method of particular solutions has been demonstrably improved by the use of (a) an improved initial nominal solution and (b) an orthogonality constraint between the Euler parameters and their corresponding costates. Furthermore, the use of a modified first-order gradient method as a "front end" for the MPS has proved to be productive for all of the spacecraft optimal attitude control problems attempted in this research.

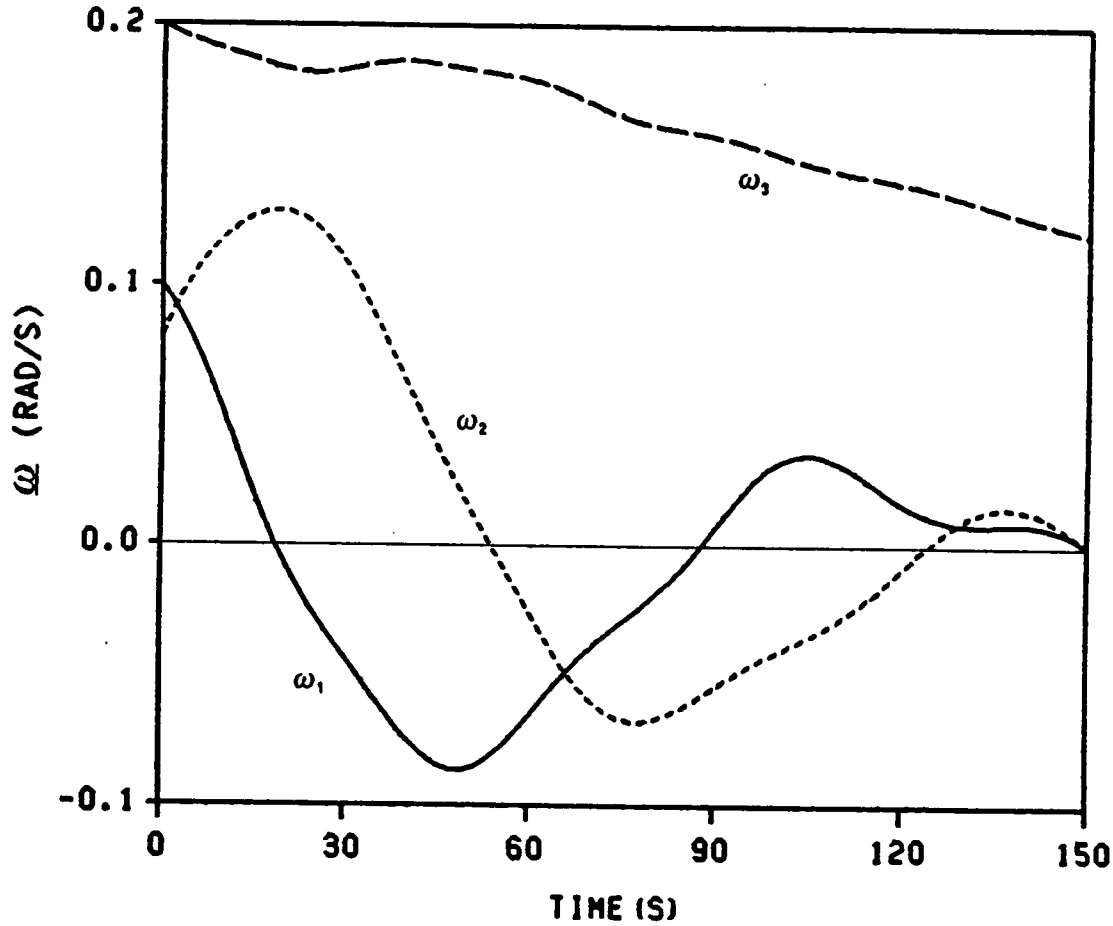

Figure 4.4 Optimal Angular Velocity for Example 4.2

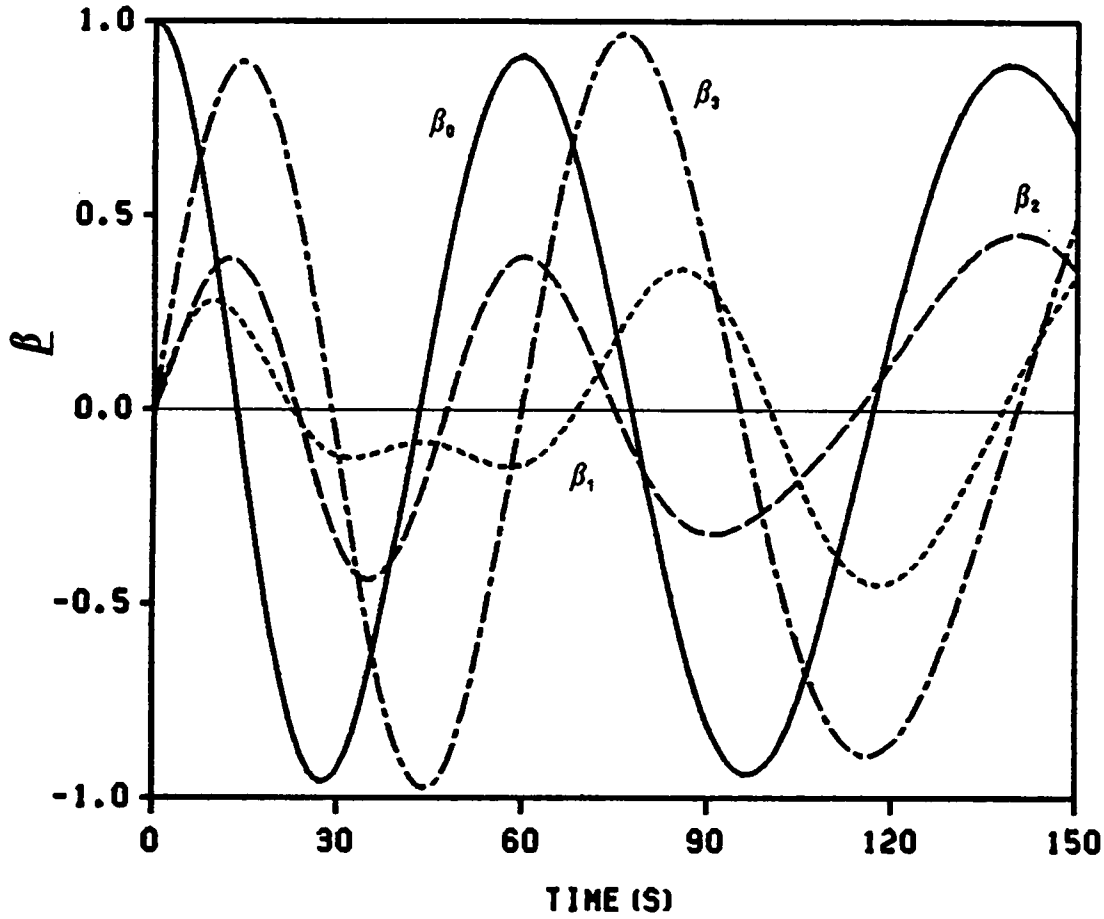

Figure 4.5 Optimal Euler Parameters for Example 4.2

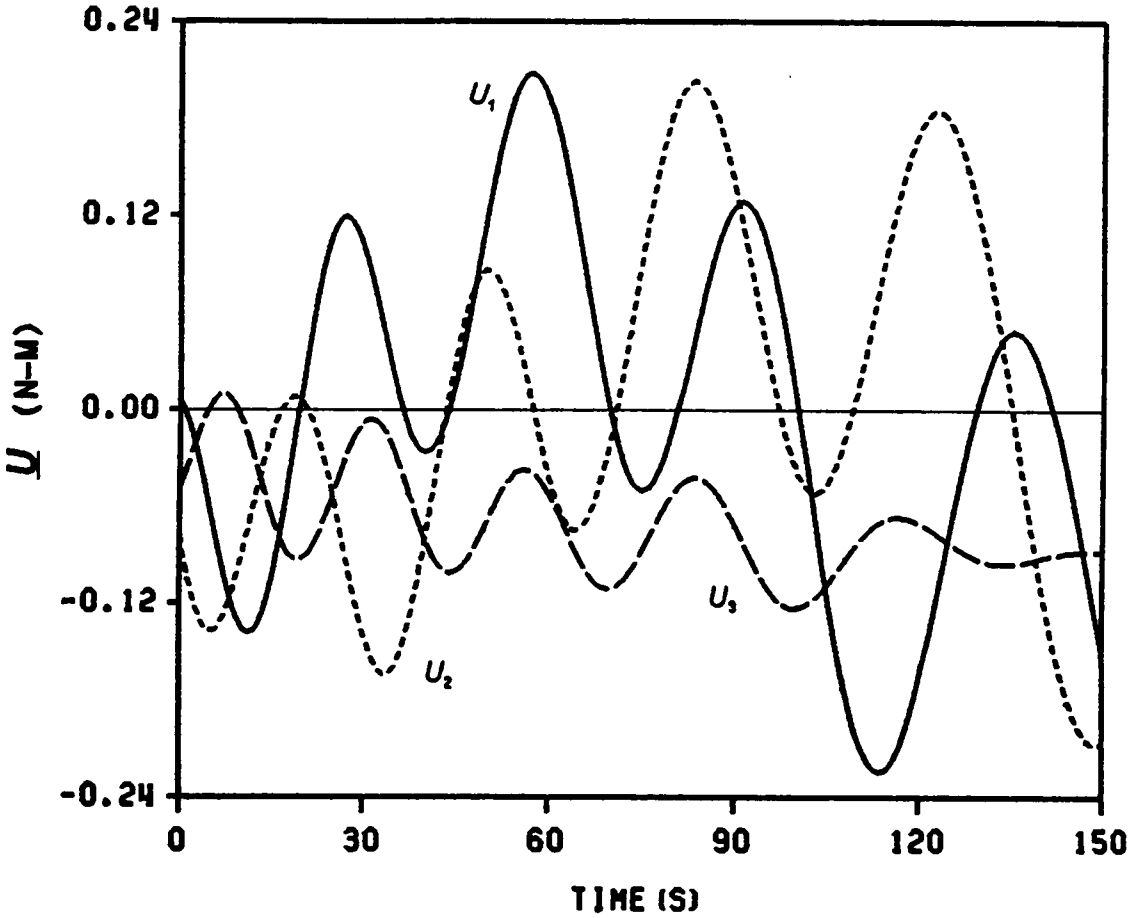

Figure 4.6 Optimal External Torque for Example 4.2

CHAPTER 5

OPTIMAL ATTITUDE MANEUVERS PROBLEMS FOR SPACECRAFT WITH REACTION WHEELS

Reaction wheels are motor-driven flywheels that can store or transfer momentum. They are used on spacecraft to add stability against disturbance torques, to provide and transfer momentum to the spacecraft body to execute slewing maneuvers, and to absorb cyclic torques. Due to the design capacity, reaction wheels are suitable for low to medium angular rate attitude maneuvers. Support and friction wear problems prevent the wheels from being very heavy or running at very high angular speeds; thus the momentum stored in the reaction wheel may eventually become so great that periodic dumping is required. A second set of torque generating devices, such as gas jets or magnetic coils, is generally required for overall angular momentum control.

Three reaction wheels is the minimum number for three-axis spacecraft attitude control. Each wheel axis may be aligned with the spacecraft principal axes. A fourth wheel is sometimes used to provide safeguard against failure of one of the orthogonal wheels. Using a reaction wheel system as a stabilizing and control device has several advantages: (1) capability of continuous high-accuracy pointing control, (2) no fuel consumption during attitude maneuvers and stability control, (3) fast, flexible response particularly good for variable spin rate control [1].

In this chapter, the optimal attitude maneuver problem of a rigid asymmetric spacecraft with a three-wheel configuration is formulated and examples are solved using the techniques discussed in the previous chapters.

5.1 Spacecraft Attitude Control with Three Reaction Wheels

Shown in Fig 5.1 [38] is a rigid asymmetric spacecraft with three reaction wheels. Each identical wheel is aligned along one of the principal axes. The total angular momentum vector can be written from Eq. (3.9) as

$$\underline{H}_C = H_1\underline{b}_1 + H_2\underline{b}_2 + H_3\underline{b}_3 \tag{5.1}$$

where

$$H_i = I_i\omega_i + I_w\Omega_i \qquad (i = 1, 2, 3) \tag{5.2}$$

and

$$I_i = I_i^* + I_w + 2J_w$$

is the component of the total principal moment of inertia of spacecraft, and

I_i^* = component of moment of inertia of the spacecraft excluding wheels
I_w = axial moment of inertia of the wheels
J_w = transverse moment of inertia of the wheels
ω_i = component of spacecraft angular velocity
Ω_i = angular rate of i^{th} wheel

The total angular momentum vector $\underline{H}_c$ is conserved in inertial space when no external torque is present. The kinetic equation (3.11) is reduced to

$$\begin{aligned}
0 &= I_1\dot{\omega}_1 + J_1\dot{\Omega}_1 + (I_3 - I_2)\omega_2\omega_3 + J_3\Omega_3\omega_2 - J_2\Omega_2\omega_3 \\
0 &= I_2\dot{\omega}_2 + J_2\dot{\Omega}_2 + (I_1 - I_3)\omega_1\omega_3 + J_1\Omega_1\omega_3 - J_3\Omega_3\omega_1 \\
0 &= I_3\dot{\omega}_3 + J_3\dot{\Omega}_3 + (I_2 - I_1)\omega_1\omega_2 + J_2\Omega_2\omega_1 - J_1\Omega_1\omega_2
\end{aligned} \tag{5.3}$$

The motor torque u_i for i^{th} wheel can be derived from

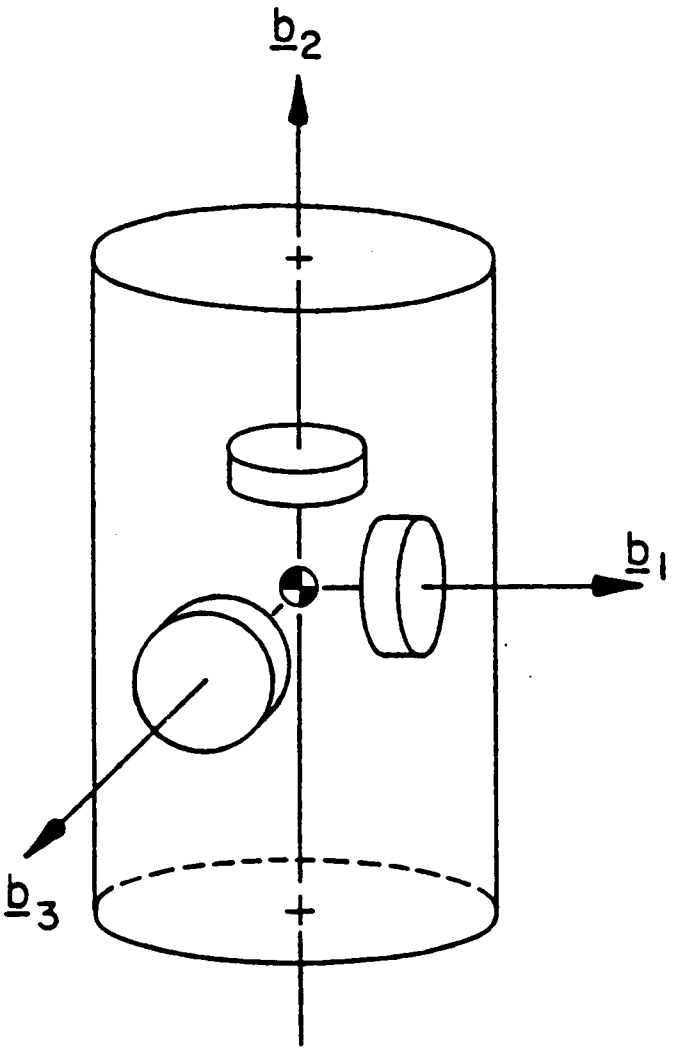

Figure 5.1 Rigid Spacecraft with Three Orthogonal Reaction Wheels

$$u_i = \frac{d}{dt}[I_w(\omega_i + \Omega_i)] = I_w(\dot{\omega} + \dot{\Omega}_i) \tag{5.4}$$

Also from Eq. (5.2)

$$I_w\Omega_i = H_i - I_i\omega_i \tag{5.5}$$

Substituting Eq. (5.4) and (5.5) into Eq. (5.3) gives

$$\begin{aligned}(I_1 - I_w)\dot{\omega}_1 &= -H_3(\beta)\omega_2 + H_2(\beta)\omega_3 - u_1\\ (I_2 - I_w)\dot{\omega}_2 &= -H_1(\beta)\omega_3 + H_3(\beta)\omega_1 - u_2\\ (I_3 - I_w)\dot{\omega}_3 &= -H_2(\beta)\omega_1 + H_1(\beta)\omega_2 - u_3\end{aligned} \tag{5.6}$$

where $H_i(\beta)$ is function of $\underline{\beta}$, and

$$\dot{\underline{\beta}} = [G(\omega)]\underline{\beta} \tag{5.7}$$

5.2 Necessary Conditions for Optimal Attitude Maneuvers

The previous performance index is used here for minimizing the motor torques u_i of the reaction wheels:

$$J = \frac{1}{2}\int_0^{t_f}[u_1^2(t) + u_2^2(t) + u_3^2(t)]\,dt$$

From the Hamiltonian of the system

$$H = \frac{1}{2}(u_1^2 + u_2^2 + u_3^2) + \underline{\lambda}^T\dot{\underline{\omega}} + \underline{\gamma}^T\dot{\underline{\beta}}$$

where $\underline{\lambda}$ and $\underline{\gamma}$ are the seven costates or Lagrange multipliers, we again derive the following first-order necessary conditions of optimality from Eqs. (2.5) and (2.6)

$$
\begin{aligned}
\dot{\lambda}_1 &= -\frac{H_3(\beta)\lambda_2}{I_2 - I_w} + \frac{H_2(\beta)\lambda_3}{I_3 - I_w} + \frac{1}{2}(\beta_1\gamma_0 - \beta_0\gamma_1 - \beta_3\gamma_2 + \beta_2\gamma_3) \\
\dot{\lambda}_2 &= \frac{H_3(\beta)\lambda_1}{I_1 - I_w} - \frac{H_1(\beta)\lambda_3}{I_3 - I_w} + \frac{1}{2}(\beta_2\gamma_0 + \beta_3\gamma_1 - \beta_0\gamma_2 - \beta_1\gamma_3) \\
\dot{\lambda}_3 &= -\frac{H_2(\beta)\lambda_1}{I_1 - I_w} + \frac{H_1(\beta)\lambda_2}{I_2 - I_w} + \frac{1}{2}(\beta_3\gamma_0 - \beta_2\gamma_1 + \beta_1\gamma_2 - \beta_0\gamma_3) \\
\dot{\underline{\gamma}} &= [G(\omega)]\underline{\gamma} \\
u_i &= \frac{\lambda_i}{I_i - I_w} \qquad (i = 1, 2, 3)
\end{aligned}
\tag{5.8}
$$

5.3 Numerical Examples

The optimal detumbling problem for the spacecraft with reaction wheels was used here to test the same solution strategies presented in Chapter 4. Given in Example 5.1 is an initially tumbling rigid spacecraft which has three identical symmetric wheels aligned along each principal axis of the spacecraft, and the angular speeds of the wheels are zero initially. The conditions of Example 5.1 listed in Table 5.1 show that the spacecraft moments of inertia, initial orientation, final orientation, and initial angular velocity used are similar to those of motion-to-rest case in Example 4.1. Listed in Table 5.2 are the iteration results using the MPS with the four strategies presented in Chapter 4 for solving Example 5.1 under different control periods. Strategy 1 and 2 could only solve the 60-second case, while Strategy 4 managed to solve all but the 100-second maneuver case. This is a clear indication that the usage of the orthogonality condition, Eq. (4.10), between the state $\underline{\beta}$ and the costate $\underline{\gamma}$ has substantially increased the convergence rate.

Table 5.1 Test Cases for Optimal Detumbling Maneuvers

Example 5.1 Detumbling of Spacecraft with Three Reaction Wheels

Spacecraft

Body Moments of Inertia (kg-m^2)		$I_1^* = 100$	$I_2^* = 115$	$I_3^* = 136$
Initial Angular Velocities (rad/s)		$\omega_1 = 0.03$	$\omega_2 = -0.03$	$\omega_3 = 0.06$
Final Angular Velocities (rad/s)		$\omega_1 = 0$	$\omega_2 = 0$	$\omega_3 = 0$
Initial Euler Parameters	$\beta_0 = 1.$	$\beta_1 = 0$	$\beta_2 = 0$	$\beta_3 = 0$
Final Euler Parameters	$\beta_0 = 0.70711$	$\beta_1 = 0.35355$	$\beta_2 = 0.35355$	$\beta_3 = 0.5$

Reaction Wheels

Wheel Axial Moment of Inertia (kg-m^2)		$I_w = 0.05$	
Wheel Transverse Moment of Inertia (kg-m^2)		$J_w = 0.025$	
Initial Wheel Angular Rates (rad/s)	$\Omega_1 = 0.$	$\Omega_2 = 0.$	$\Omega_3 = 0.$

Final Wheel Angular Rates: unspecified

Final Maneuver Time: from 20 to 100 seconds

I_i^* : Principal moments of inertia of spacecraft excluding wheels.

Table 5.2 Comparison of Strategies for Example 5.1

Strategy	Maneuver Time (s)	No. of Iterations	Convergence
1	20	-	No
	40	-	No
	60	9	Yes
	80	-	No
	100	-	No
2	20	-	No
	40	-	No
	60	7	Yes
	80	-	No
	100	-	No
3	20	-	No
	40	-	No
	60	4	Yes
	80	13	Yes
	100	-	No
4	20	3	Yes
	40	4	Yes
	60	4	Yes
	80	7	Yes
	100	-	No
Hybrid	100	30 FOGM/7 MPS	Yes

The 100-second maneuver case was successfully solved by the hybrid method with 30 FOGM and 7 MPS iterations. The same final penalty matrix, the weight of 1000 for ω_i and 100 for β_j, used in Example 4.1 was used here again with control step size fixed at 0.007. Shown in Fig.5.2 through 5.5 are the 100-second trajectories of angular velocity, attitude, wheel velocities, and internal torques with each figure indicating (a) the initial nominal solution with Strategy 4 for the MPS, (b) the initial nominal solution for the hybrid method, (c) the trajectory at switching time in the hybrid method, and (d) the final optimal trajectory. From these figures, we can also conclude that the trajectory at switching time in the hybrid method is a better approximation to the optimal trajectory than the one generated by Strategy 4.

5.4 Concluding Remarks

The results shown in Table 5.2 indicate that the trend of convergence is similar to that of the externally torqued spacecraft problems of Chapter 4 as the improvement strategies are applied. However, the maneuver times which can be solved for spacecraft with internal reaction wheels control problems are shorter than those of externally torqued cases under similar boundary conditions. The difficulty of solving spacecraft attitude control problem with reaction wheels is due to the extra constraint condition that the magnitude of total angular momentum H_c is constant during the control period. This constraint, which makes the time rate of change of angular velocity explicitly dependent upon the Euler parameters in the system equations, further strengthens the nonlinear coupled effects among the state-costate equations and causes the iteration process to diverge more easily. Nevertheless, the example given in this chapter has high initial angular velocity and should be a limiting case for control devices using reaction wheels. Because the moment of inertia of the wheels

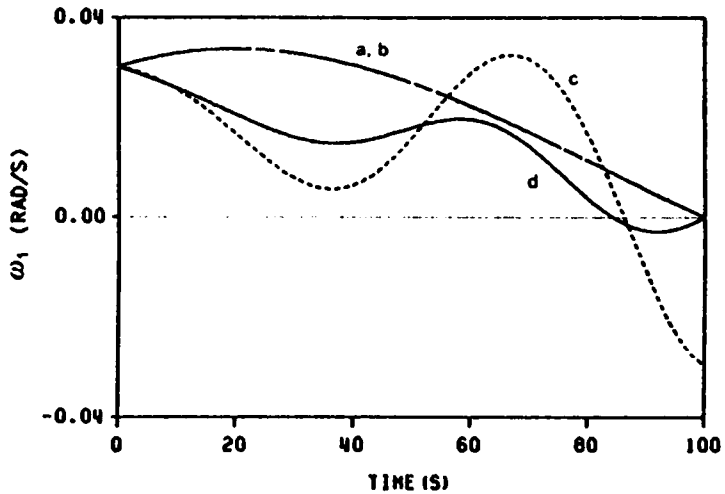

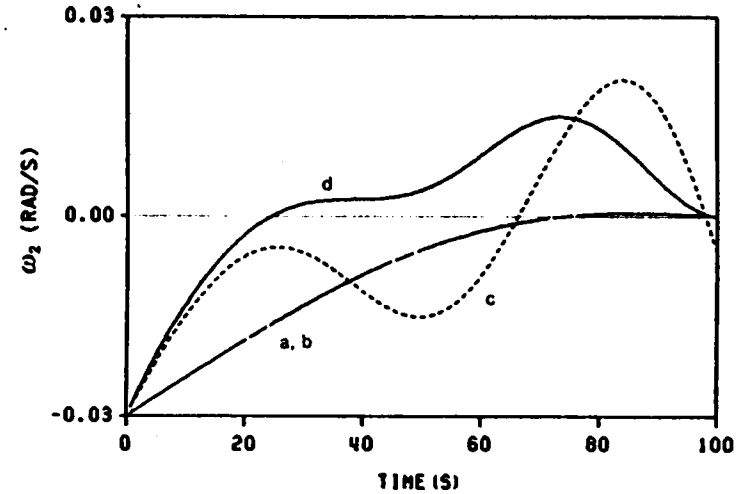

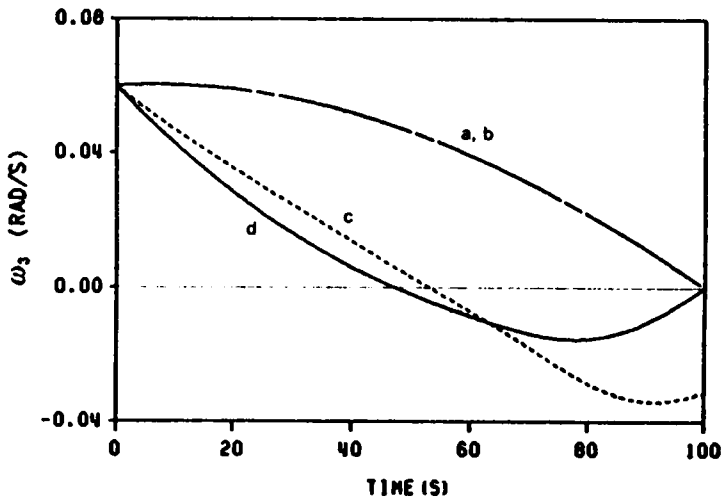

Figure 5.2 Comparison of 100-Second Angular Velocities for Example 5.1

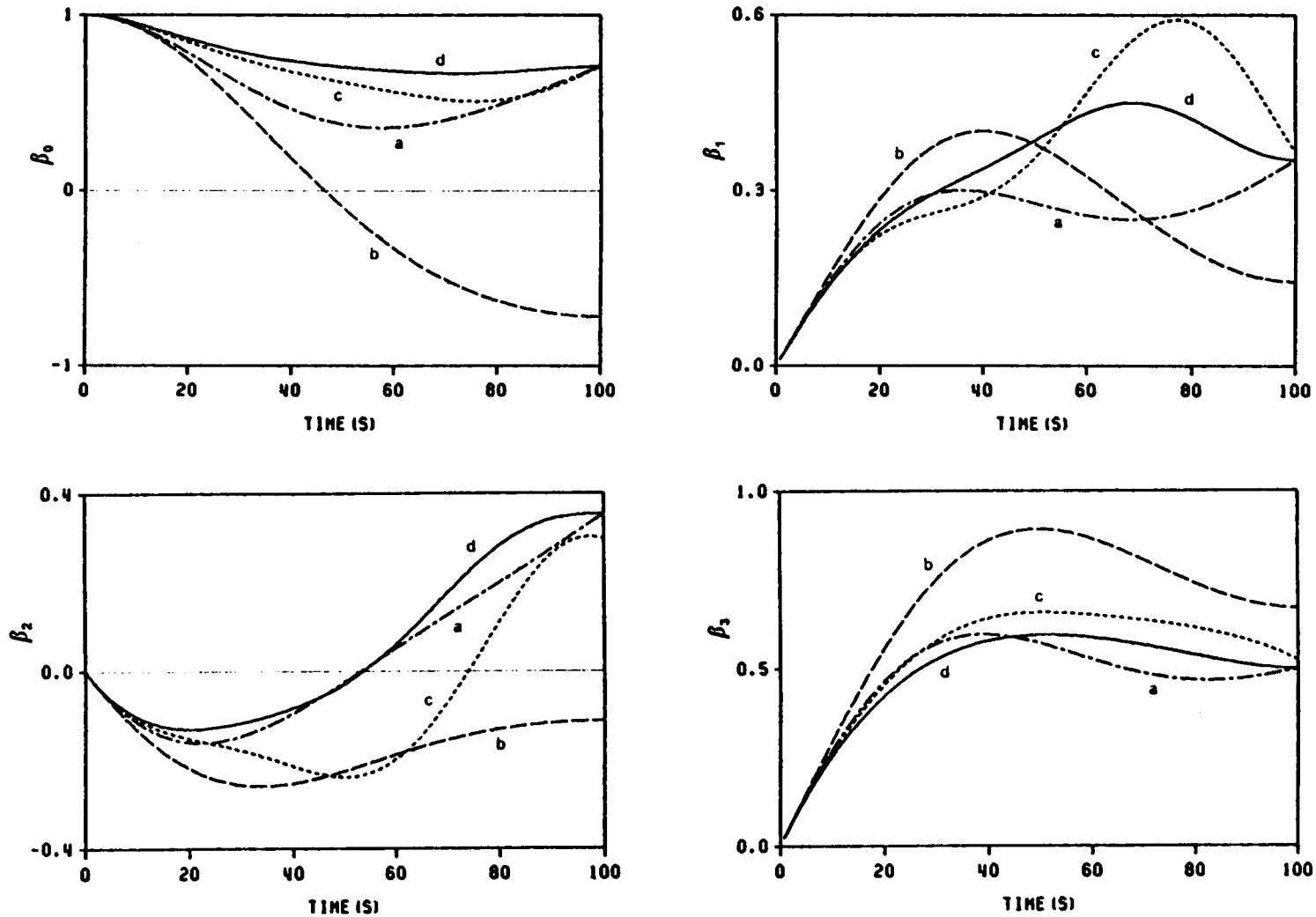

Figure 5.3 Comparison of 100-Second Euler Parameters for Example 5.1

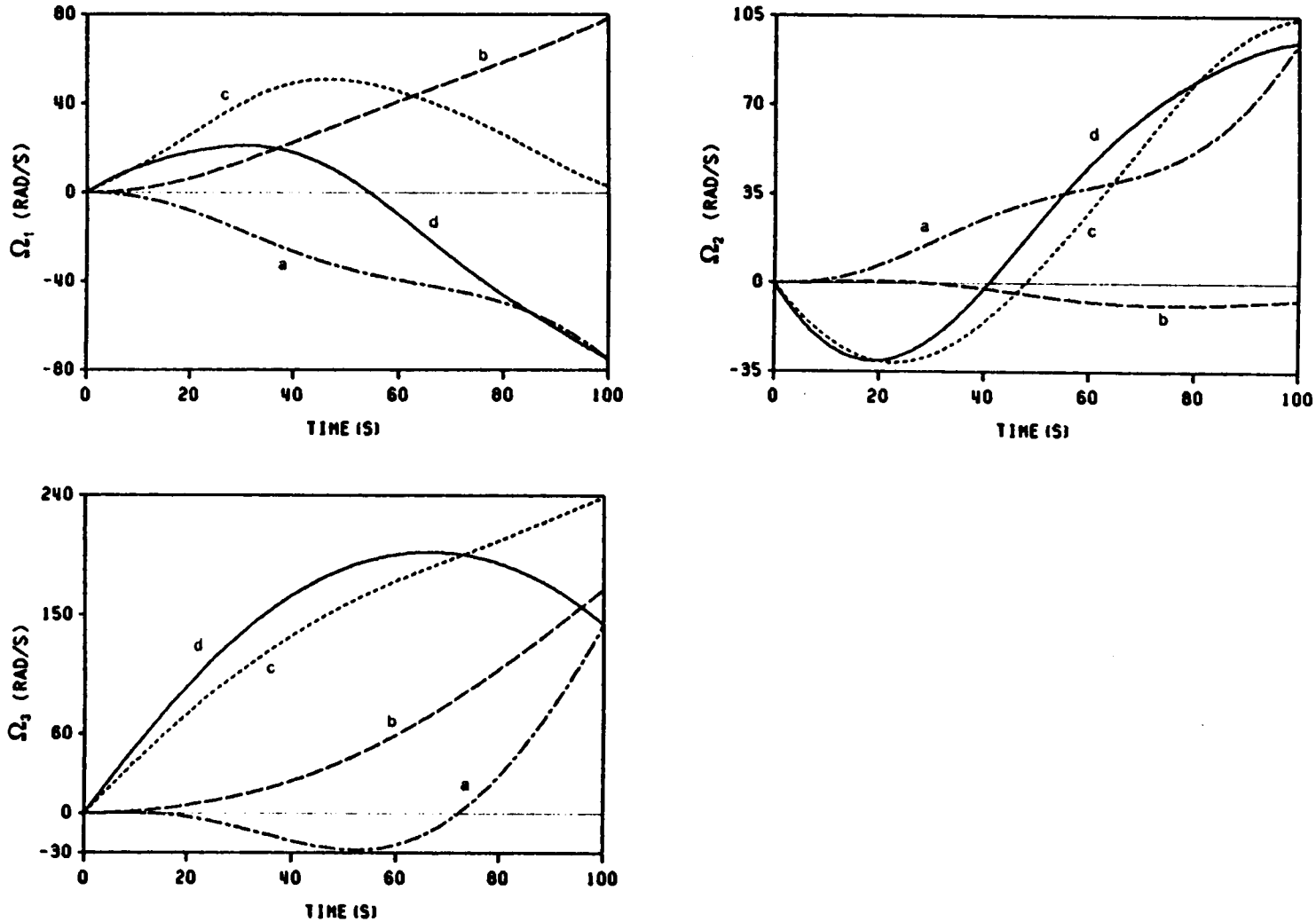

Figure 5.4 Comparison of 100-Second Wheel Velocities for Example 5.1

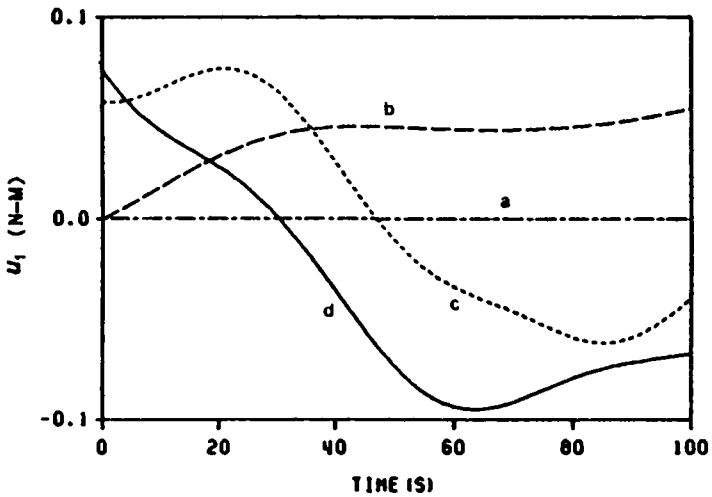

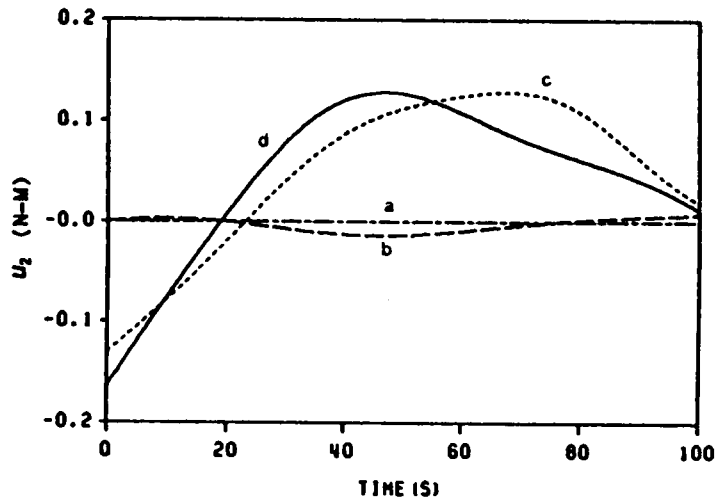

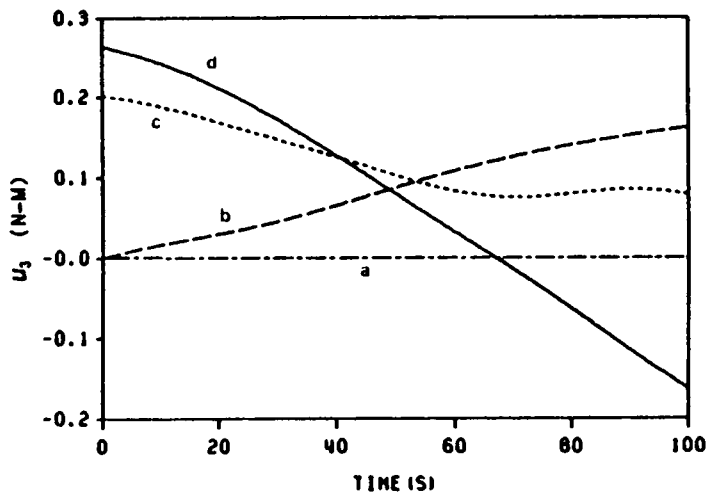

Figure 5.5 Comparison of 100-Second Internal Torques for Example 5.1

is small, it requires a high wheel speed or long control period to maneuver the spacecraft. The first is physically impractical for the wheel design and the second makes the optimal control problem more difficult to solve.

CHAPTER 6

REAL-TIME NEAR-OPTIMAL GUIDANCE STRATEGY

In the presence of unknown input disturbances and measurement errors, the system states may deviate from the optimal trajectory generated by the open-loop control introduced previously. To correct the errors, a near-optimal guidance control strategy is presented in this chapter which tracks the given optimal trajectory during the maneuver. This neighboring optimal guidance scheme [39,40,41], which takes the perturbed states to the specified terminal manifold and minimizes the perturbed performance index, can be applied in real-time whenever the errors occur.

Through linearization of the original nonlinear dynamic equations and the performance index about a given optimal trajectory, a typical guidance control problem can be solved by the method of particular solutions in one single iteration. A tracking example is also given which shows that highly accurate tracking results can be achieved.

6.1 Problem Formulation

Consider a dynamical system described by the following vector differential equation

$$\dot{\underline{x}}(t) = \underline{f}(\underline{x}(t), \underline{u}(t), t) \tag{6.1}$$

moving along an optimal trajectory with the boundary conditions $\underline{x}(0)$ and $\underline{x}(t_f)$ with and the final time t_f specified. The state $\underline{x}(t)$, an n-dimensional vector, and control

function $\underline{u}(t)$, an m-dimensional vector, must satisfy the system equation and the first-order necessary conditions of optimality

$$(\dot{\underline{\lambda}})^T = -\frac{\partial H}{\partial \underline{x}}$$
$$\frac{\partial H}{\partial \underline{u}} = 0$$

The augmented cost functional is written as

$$J = \int_0^{t_f} [H - \underline{\lambda}^T \dot{\underline{x}}]\, dt$$

where the system Hamiltonian H is defined as in Eq. (2.4). Suppose small state errors $\underline{w}(t_1)$ are measured at time t_1, where $0 < t_1 < t_f$. Our goal is to develop a real-time control law which eliminates the errors at t_f while following the optimal trajectory closely. Although the guidance problem can be one with free final boundary conditions and variable final time [42,43], we consider the formulation for fixed final boundary conditions and fixed final time. Let the perturbed quantities be

$$\underline{x}(t) = \tilde{\underline{x}}(t) + \underline{w}(t)$$
$$\underline{u}(t) = \tilde{\underline{u}}(t) + \underline{v}(t)$$

where $\tilde{\underline{x}}$ and $\tilde{\underline{u}}$ are the optimal state and control vectors, respectively. The $\underline{w}(t)$ and $\underline{v}(t)$ are understood to be the state and control perturbations $\delta\underline{x}(t)$ and $\delta\underline{u}(t)$ which satisfy the variational differential equation

$$\dot{\underline{w}}(t) = \tilde{f}_x \underline{w}(t) + \tilde{f}_u \underline{v}(t) \tag{6.2}$$

where

$$\tilde{f}_x = \frac{\partial f(\tilde{\underline{x}}, \tilde{\underline{u}})}{\partial \underline{x}} , \qquad \tilde{f}_u = \frac{\partial f(\tilde{\underline{x}}, \tilde{\underline{u}})}{\partial \underline{u}}$$

Assuming that all the functions are twice differentable and that $\partial^2 H/\partial u^2$ is non-singular [44], we can expand the augmented cost functional by a Taylor's series expansion to second order along an optimal trajectory

$$J(\tilde{\underline{x}} + \underline{w}, \tilde{\underline{u}} + \underline{v}) = J(\tilde{\underline{x}}, \tilde{\underline{u}}) + \frac{1}{2} \int_{t_1}^{t_f} [\underline{w}^T \tilde{H}_{xx} \underline{w} + 2\underline{w}^T \tilde{H}_{xu} \underline{v} + \underline{v}^T \tilde{H}_{uu} \underline{v}] \, dt \tag{6.3}$$

where the first-order terms are dropped as they satisfy the first-order necessary conditions of optimality, and

$$\tilde{H}_{xx} = \frac{\partial^2 H(\tilde{\underline{x}}, \tilde{\underline{u}})}{\partial \underline{x}^2} , \qquad \tilde{H}_{xu} = \frac{\partial^2 H(\tilde{\underline{x}}, \tilde{\underline{u}})}{\partial \underline{x} \partial \underline{u}} , \qquad \tilde{H}_{uu} = \frac{\partial^2 H(\tilde{\underline{x}}, \tilde{\underline{u}})}{\partial \underline{u}^2}$$

Instead of minimizing the original cost functional, we now minimize the second-order perturbed quantities of the cost functional from t_1 to t_f , The augmented variational cost functional is defined as

$$J_2 = \int_{t_1}^{t_f} [H_2 - \underline{\xi}^T \dot{\underline{w}}] dt \tag{6.4}$$

where H_2 is the Hamiltonian of the perturbed system and is defined as

$$H_2 = \frac{1}{2} (\underline{w}^T \tilde{H}_{xx} \underline{w} + 2\underline{w}^T \tilde{H}_{xu} \underline{v} + \underline{v}^T \tilde{H}_{uu} \underline{v}) + \underline{\xi}^T (\tilde{f}_x \underline{w} + \tilde{f}_u \underline{v})$$

The $\underline{\xi}$ is the variational costate vector. Through the calculus of variations or Pontryagin's Principle, the variational costate equation is

$$\dot{\underline{\xi}} = -\tilde{H}_{xx}\underline{w} - \tilde{f}_x^T\underline{\xi} - \tilde{H}_{xu}\underline{v} \tag{6.5}$$

and the optimality condition is

$$\tilde{H}_{xu}\underline{w} + \tilde{f}_u^T\underline{\xi} + \tilde{H}_{uu}\underline{v} = 0 \tag{6.6}$$

or the perturbation control function can be written as

$$\underline{v} = -\tilde{H}_{uu}^{-1}(\tilde{H}_{xu}\underline{w} + \tilde{f}_u^T\underline{\xi}) \tag{6.7}$$

The formulation becomes one of solving the accessory minimum problem associated with the calculus of variations. However, the assumptions that the problem satisfies the strong form of the Legendre-Clebsch condition and possesses no conjugate point over the entire interval are made [45,46]. Substitution of Eq. (6.7) into Eqs. (6.2) and (6.5) yields

$$\begin{aligned} \dot{\underline{w}}(t) &= A(t)\underline{w}(t) - B(t)\underline{\xi}(t) \\ \dot{\underline{\xi}}(t) &= -C(t)\underline{w}(t) - A(t)^T\underline{\xi}(t) \end{aligned} \tag{6.8}$$

where

$$\begin{aligned} A(t) &= \tilde{f}_x - \tilde{f}_u\tilde{H}_{uu}^{-1}\tilde{H}_{ux} \\ B(t) &= \tilde{f}_u\tilde{H}_{uu}^{-1}\tilde{f}_u^T \\ C(t) &= \tilde{H}_{xx} - \tilde{H}_{xu}\tilde{H}_{uu}^{-1}\tilde{H}_{ux} \end{aligned}$$

The system equations are linear with time-varying coefficient matrices. Equation (6.8) with the boundary conditions

$$\underline{w}(t_1) = \underline{w}_1 \quad , \quad \underline{w}(t_f) = 0 \tag{6.9}$$

is a linear two-point boundary-value problem.

6.2 Near-Optimal Guidance Algorithm

The linear two-point boundary-value problem can be easily solved by the method of particular solutions in one iteration [26]. Now that $\underline{x}(t)$ is a n x 1 vector, we need a set of n+1 particular solutions to form the solution of Eq. (6.8). Following the formulation given in Chapter 2, we define n+1 particular solutions

$$\underline{p}_j = \underline{p}_j(t), \quad j = 1, 2, ..., n+1$$

which are obtained by forward integration of Eq. (6.8) from t_1 to t_f subject to the conditions

$$\begin{aligned} w_j^i(t_1) &= w^i \quad j = 1, 2, ..., n+1 \ , \quad i = 1, 2, ..., n \\ \xi_j^i(t_1) &= \delta_{jk} \quad j = 1, 2, ..., n+1 \ , \quad k = 1, 2, ..., n \end{aligned} \tag{6.10}$$

where w^i is the i^{th} element of the initial boundary vector $\underline{w}(t_1)$ and δ_{jk} denotes the Kronecker delta. Simple substitution will show that the linear combination of the n+1 particular solutions

$$\underline{p}(t) = \sum_{j=1}^{n+1} k_j \underline{p}_j(t) \tag{6.11}$$

does indeed satisfy Eq. (6.8). Substituting boundary conditions into Eq. (6.11), we can determine the n+1 scalar constants k_j from the following n+1 linear algebraic equations

$$\sum_{j=1}^{n+1} k_j = 1 \quad \text{and} \quad \sum_{j=1}^{n+1} k_j p_j^i(t_f) = 0 \qquad i = 1, 2, \ldots, n$$

6.3 Spacecraft Attitude Guidance Maneuvers

The rigid externally-torqued spacecraft given in Example 4.1 is used again here for Example 6.1. The same state boundary conditions are used for a 60-second maneuver. Assume that the state errors shown in Table 6.1 are measured at t= 10 seconds. Note that the introduced errors at t= 10 seconds are 10% of each optimal angular velocity component and 5% of each optimal Euler parameter. The guidance effort is to generate a neighboring optimal trajectory which takes the perturbed states to the desired final state boundary conditions while minimizing the perturbed cost functional. The parameter matrices A(t), B(t), and C(t) in Eq. (6.8) are calculated from the following system matrices:

$$\tilde{f}_x = \begin{bmatrix} 0 & -J_1\omega_3 & -J_1\omega_2 & 0 & 0 & 0 & 0 \\ -J_2\omega_3 & 0 & -J_2\omega_1 & 0 & 0 & 0 & 0 \\ -J_3\omega_2 & -J_3\omega_1 & 0 & 0 & 0 & 0 & 0 \\ -\frac{1}{2}\beta_1 & -\frac{1}{2}\beta_2 & -\frac{1}{2}\beta_3 & 0 & -\frac{1}{2}\omega_1 & -\frac{1}{2}\omega_2 & -\frac{1}{2}\omega_3 \\ \frac{1}{2}\beta_0 & -\frac{1}{2}\beta_3 & \frac{1}{2}\beta_2 & \frac{1}{2}\omega_1 & 0 & \frac{1}{2}\omega_3 & -\frac{1}{2}\omega_2 \\ \frac{1}{2}\beta_3 & \frac{1}{2}\beta_0 & -\frac{1}{2}\beta_1 & \frac{1}{2}\omega_2 & -\frac{1}{2}\omega_3 & 0 & \frac{1}{2}\omega_1 \\ -\frac{1}{2}\beta_2 & \frac{1}{2}\beta_1 & \frac{1}{2}\beta_0 & \frac{1}{2}\omega_3 & \frac{1}{2}\omega_2 & -\frac{1}{2}\omega_1 & 0 \end{bmatrix}$$

Table 6.1 State Conditions at Time = 10 Seconds for Example 6.1

Example 6.1 Real-Time Near-Optimal Guidance Problem

	Optimal States	Perturbed States		State Errors
ω_1	0.03945	0.04335	$\delta\omega_1$	0.00390
ω_2	-0.00328	-0.00361	$\delta\omega_2$	-0.00033
ω_3	0.03702	0.04072	$\delta\omega_3$	0.00370
β_0	0.94367	0.93886	$\delta\beta_0$	-0.00481
β_1	0.21331	0.22161	$\delta\beta_1$	0.00830
β_2	-0.09830	-0.10375	$\delta\beta_2$	-0.00545
β_3	0.23360	0.24272	$\delta\beta_3$	0.00912

$$\tilde{f}_u^T = \begin{bmatrix} \frac{1}{I_1} & 0 & 0 & 0 & 0 & 0 & 0 \\ 0 & \frac{1}{I_2} & 0 & 0 & 0 & 0 & 0 \\ 0 & 0 & \frac{1}{I_2} & 0 & 0 & 0 & 0 \end{bmatrix}$$

$$\tilde{H}_{uu} = \begin{bmatrix} 1 & 0 & 0 \\ 0 & 1 & 0 \\ 0 & 0 & 1 \end{bmatrix}$$

$$\tilde{H}_{xx} = \begin{bmatrix} 0 & -J_3\lambda_3 & -J_2\lambda_2 & \frac{1}{2}\gamma_1 & -\frac{1}{2}\gamma_0 & -\frac{1}{2}\gamma_3 & \frac{1}{2}\gamma_2 \\ -J_3\lambda_3 & 0 & -J_1\lambda_1 & \frac{1}{2}\gamma_2 & \frac{1}{2}\gamma_3 & -\frac{1}{2}\gamma_0 & -\frac{1}{2}\gamma_1 \\ -J_2\omega_2 & -J_1\lambda_1 & 0 & \frac{1}{2}\gamma_3 & -\frac{1}{2}\gamma_2 & \frac{1}{2}\gamma_1 & -\frac{1}{2}\gamma_0 \\ \frac{1}{2}\gamma_1 & \frac{1}{2}\gamma_2 & \frac{1}{2}\gamma_3 & 0 & 0 & 0 & 0 \\ -\frac{1}{2}\gamma_0 & \frac{1}{2}\gamma_3 & -\frac{1}{2}\gamma_2 & 0 & 0 & 0 & 0 \\ -\frac{1}{2}\gamma_3 & -\frac{1}{2}\gamma_0 & \frac{1}{2}\gamma_1 & 0 & 0 & 0 & 0 \\ \frac{1}{2}\gamma_2 & -\frac{1}{2}\gamma_1 & -\frac{1}{2}\gamma_0 & 0 & 0 & 0 & 0 \end{bmatrix}$$

Because the control components are linear in the attitude dynamic equation (4.1), H_{ux} is a zero matrix. The integration step is taken to be 0.1 seconds for the simulations.

The iterated final states for the optimal trajectory, the near-optimal trajectory, and the perturbed trajectory are compared in Table 6.2. Shown in Figs. 6.1 through 6.10 are the angular velocity components, the Euler parameters, and the control torque components for the three trajectories.

Table 6.2 Comparison of States at Time = 60 seconds for Example 6.1

	Optimal States	Near-Optimal States	Perturbed States
ω_1	-0.01500	-0.01501	-0.01171
ω_2	0.00000	0.00003	0.00113
ω_3	0.00000	-0.00000	-0.00331
β_0	0.70711	0.70711	0.61050
β_1	0.35355	0.35305	0.39452
β_2	0.35355	0.35409	0.36378
β_3	0.50000	0.50022	0.58271

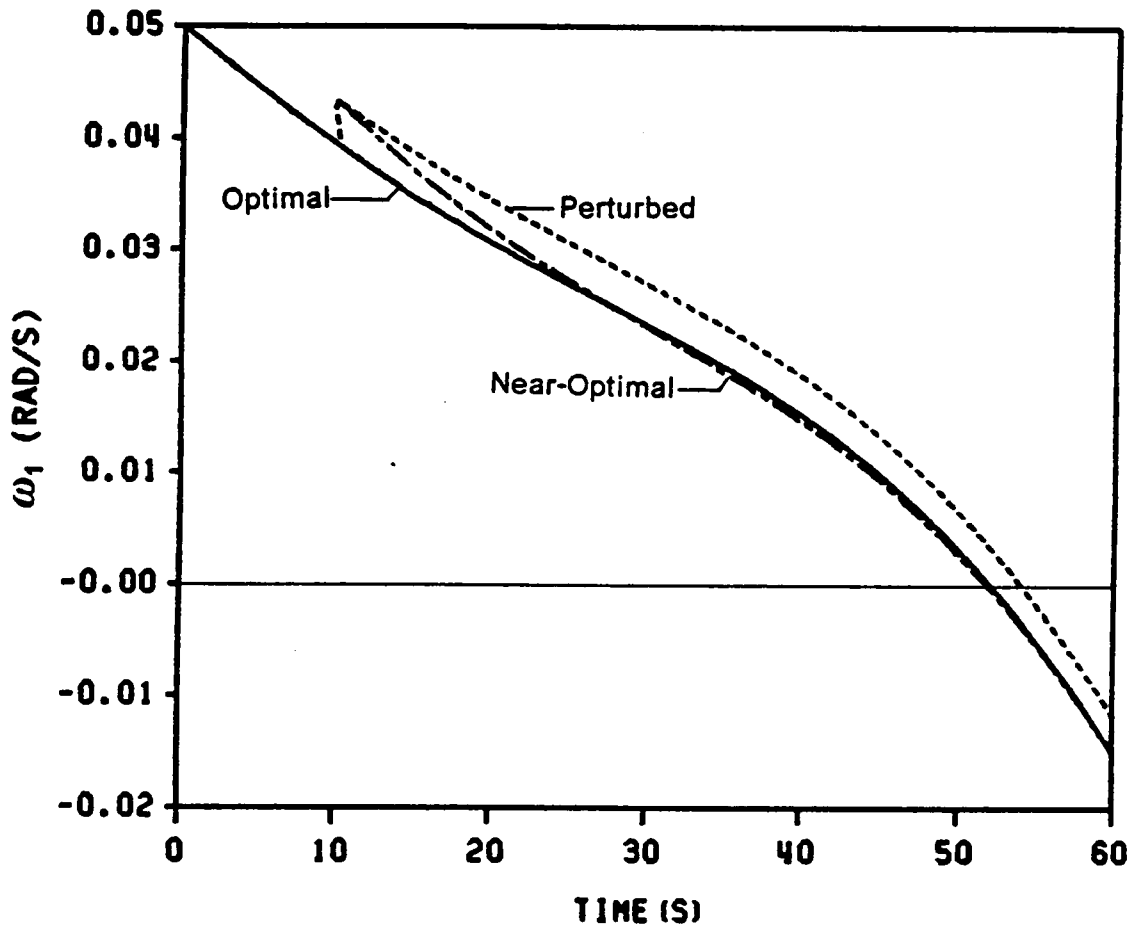

Figure 6.1 Comparison of ω_1 for Example 6.1

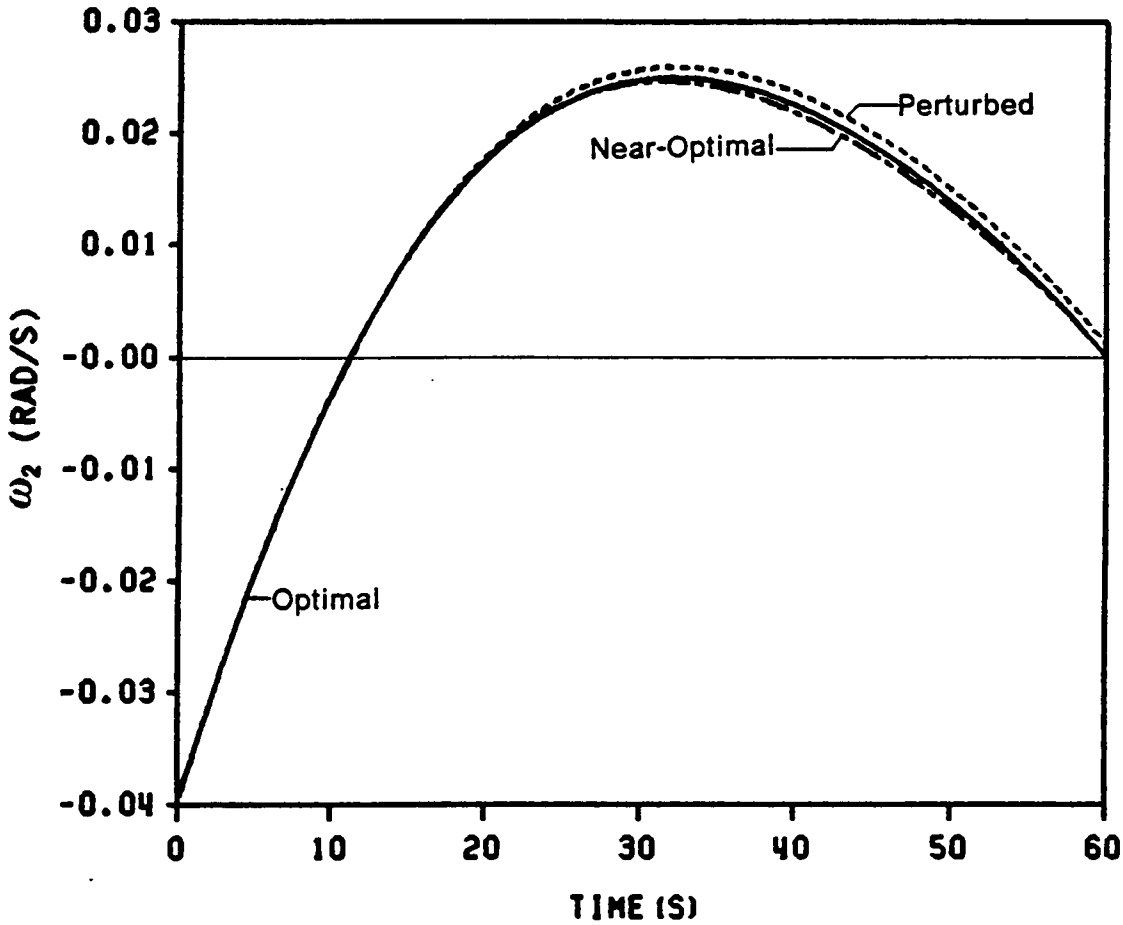

Figure 6.2 Comparison of ω_2 for Example 6.1

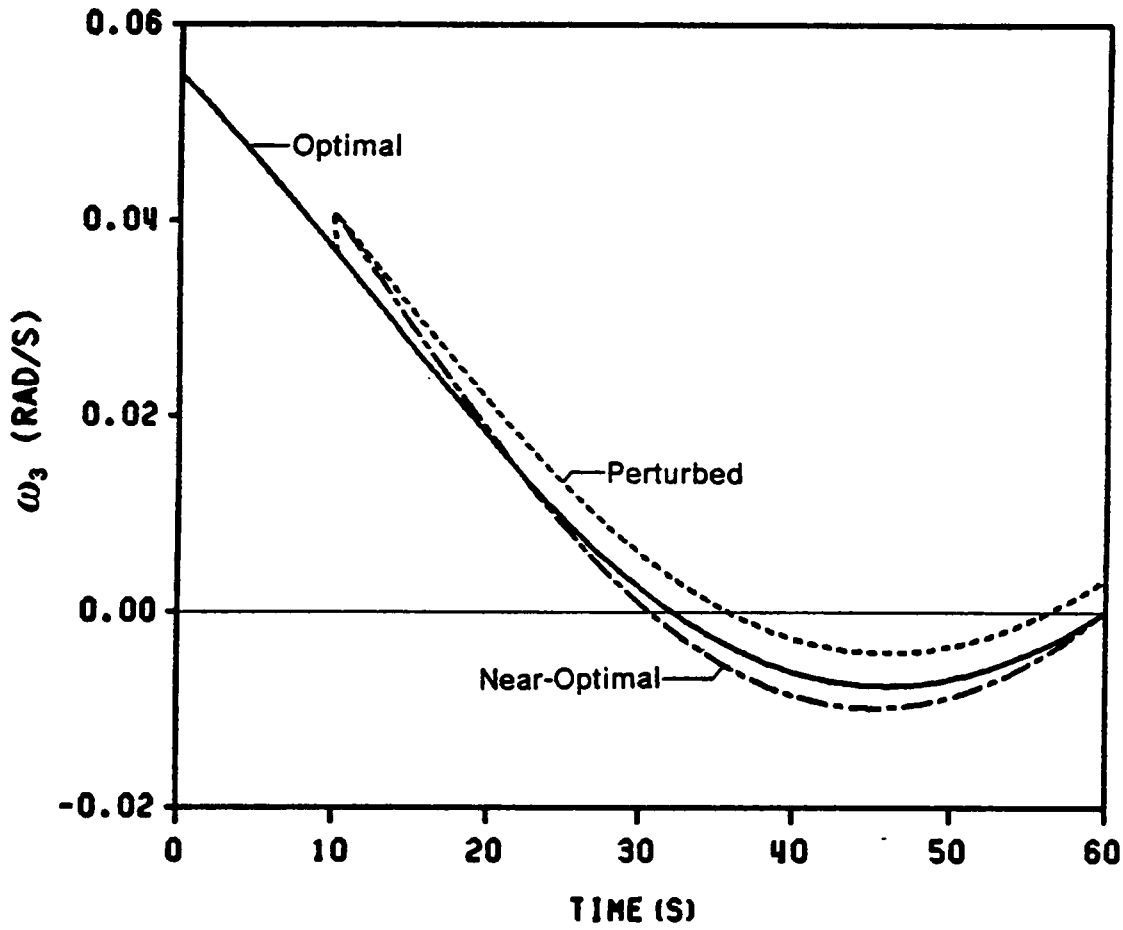

Figure 6.3 Comparison of ω_3 for Example 6.1

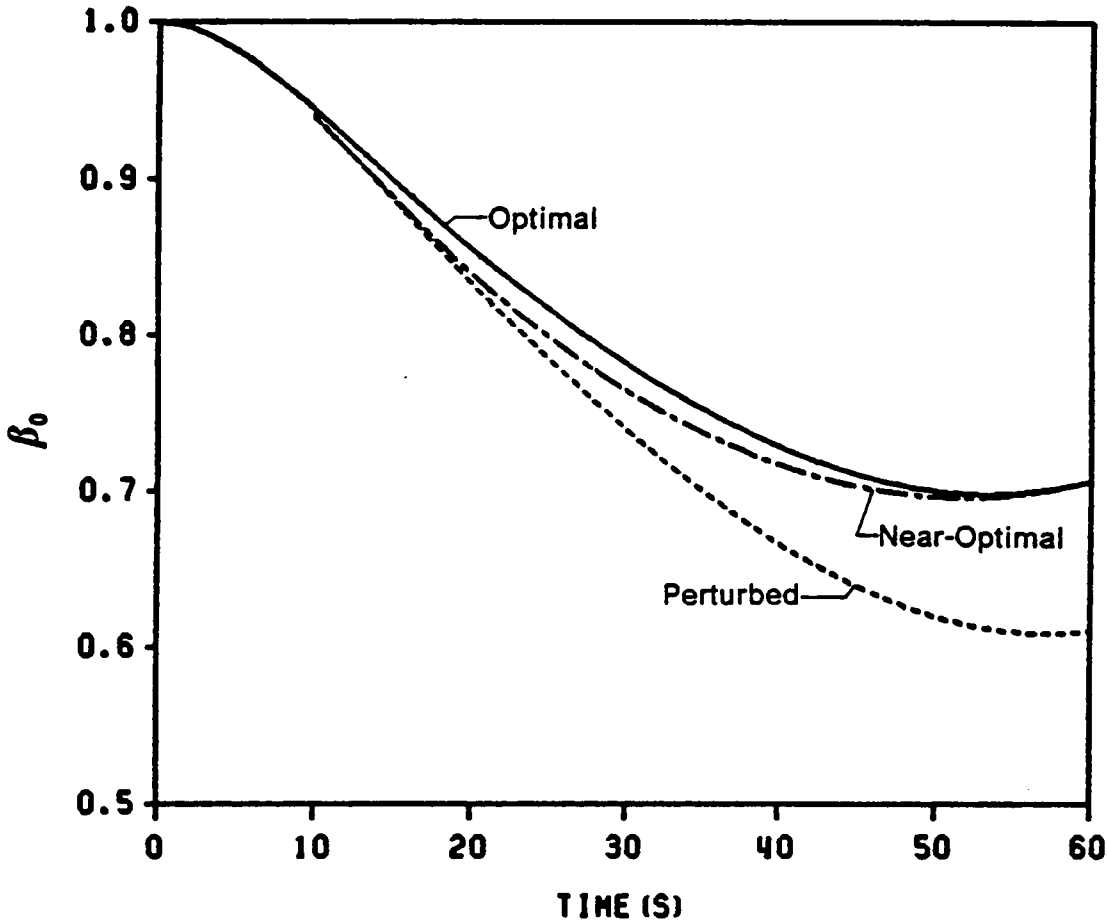

Figure 6.4 Comparison of β_0 for Example 6.1

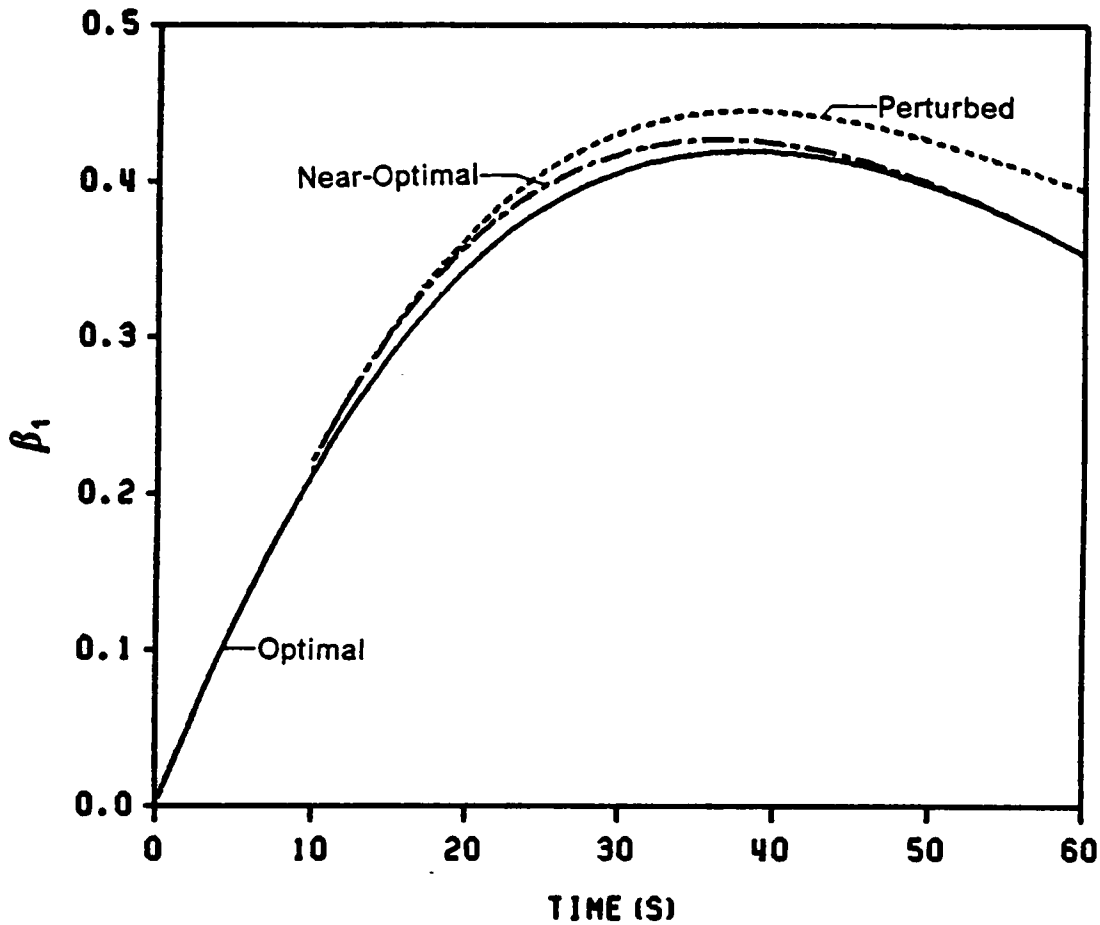

Figure 6.5 Comparison of β_1 for Example 6.1

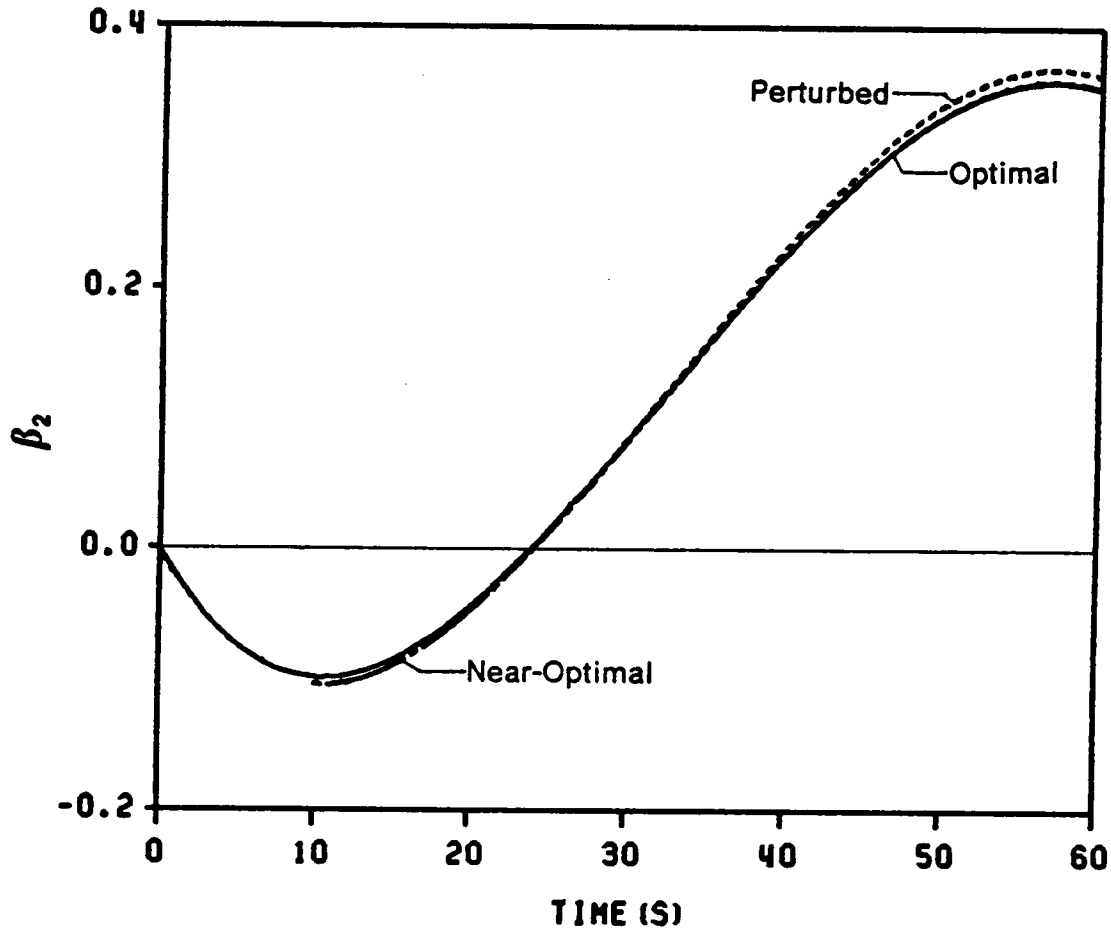

Figure 6.6 Comparison of β_2 for Example 6.1

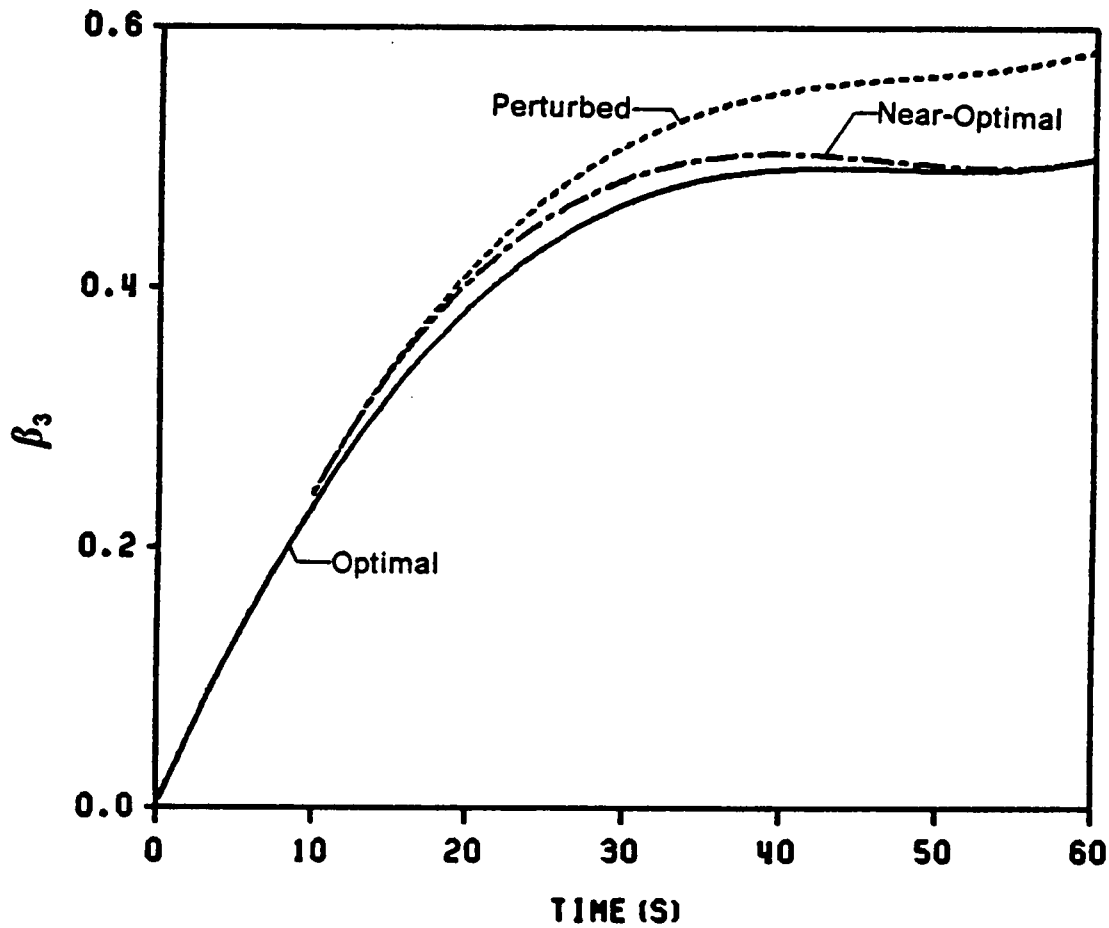

Figure 6.7 Comparison of β_3 for Example 6.1

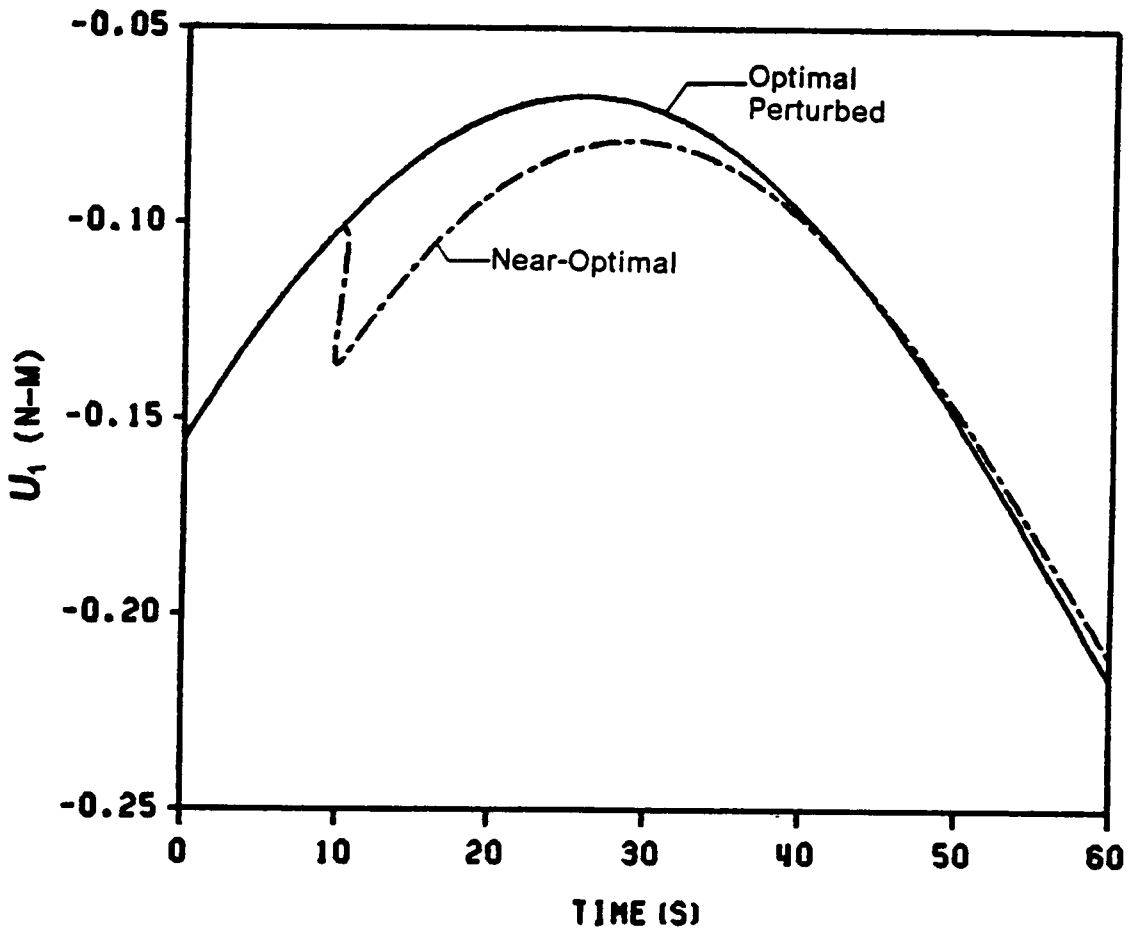

Figure 6.8 Comparison of U_1 for Example 6.1

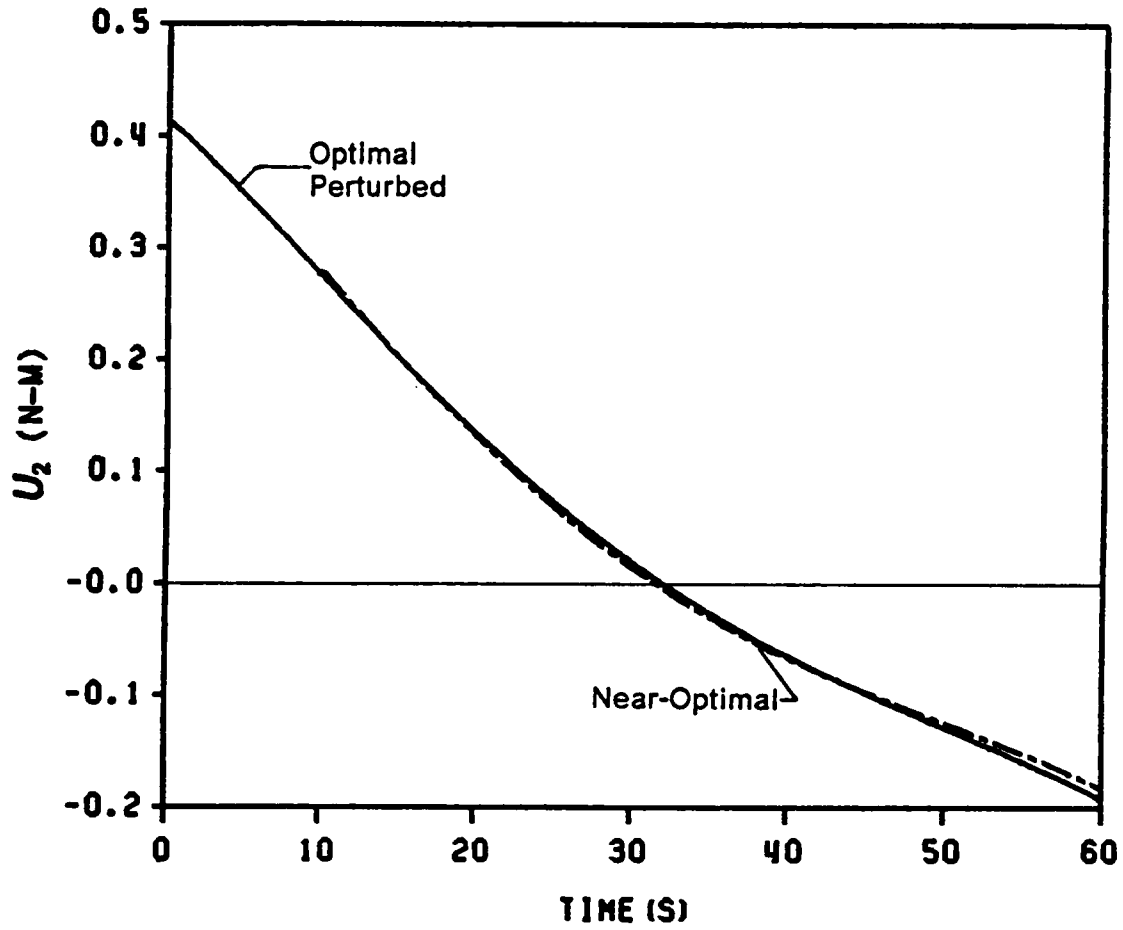

Figure 6.9 Comparison of U_2 for Example 6.1

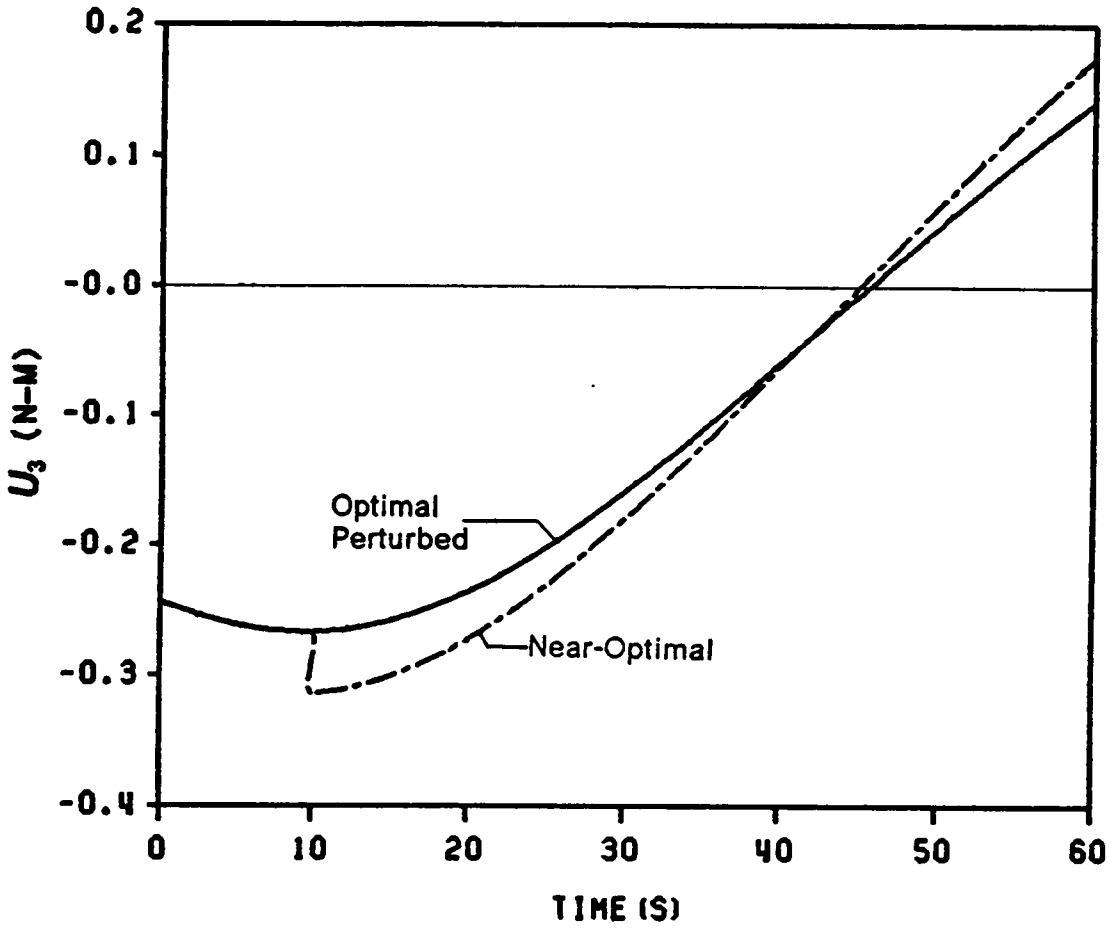

Figure 6.10 Comparison of U_3 for Example 6.1

The results shown in Table 6.2 indicate that final states errors of the near-optimal trajectory are about 0.05% in the angular velocity components and 0.1% in the orientation parameters, whereas in the perturbed trajectory these errors are 22% and 15%, respectively.

6.4 Concluding Remarks

The effectiveness of the real-time near-optimal guidance strategy has been demonstrated through Example 6.1. To implement the guidance scheme in real time, the following procedures can be taken [46]: (1) integrate the unperturbed equations of motion from t_1 to $t_1 + \Delta t_1$, where Δt_1 is the amount of time for computing a new control, according to the perturbed state $\underline{x}(t_1) + \delta\underline{x}(t_1)$ using the last control $\tilde{\underline{u}}(t)$; (2) after completion of the computation, the near-optimal control will be punctually started at $t_1 + \Delta t_1$. As the Δt_1 is fairly small when a good mission computer is used, we can consider the process equivalent to a feedback control process. Numerically, the final state errors in the near-optimal trajectory can be further reduced by either reducing the guidance control period or the integration step, or both. The simulation results also indicate that the sensitivity of the differential equations due to variations in the initial states is remarkably small and the controllability region could be quite large. A large set of neighboring optimal control trajectories covering all the possible maneuver cases can be generated in real time from a carefully determined and pre-calculated set of optimal trajectories.

CHAPTER 7

CONCLUSIONS AND RECOMMENDATIONS

Several direct and indirect iteration methods for solving the NTBVP associated with optimal control problems have been discussed. Four improvement strategies for the indirect method of particular solutions were proposed with the emphasis in formulation of good starting solutions. Comparison of the strategies was made through examples of externally and internally torqued rigid asymmetric spacecraft general large-angle attitude maneuvers. Numerical results indicate that Strategy 4 is the most reliable one among the strategies in approximating optimal trajectories with a lesser degree of nonlinearity. A hybrid approach coupling the modified first-order gradient method with the method of particular solutions has shown the best results in solving all the given examples including strongly nonlinear test cases that could not be solved by any of the four strategies. A real-time near-optimal guidance scheme is also proposed. The effectiveness of the scheme was demonstrated through formulating a neighboring optimal trajectory which takes the perturbed states to the desired manifold by tracking a given optimal trajectory.

Based on the computing methods presented, we can design an efficient off-line trajectory planning and on-line guidance logic. Optimal trajectories with different combinations of boundary conditions are precalculated and stored in an on-board computer, which then applies the guidance scheme using the precalculated trajectories as bases to form neighboring trajectories. Ideally, a very broad set of sub-optimal trajectories covering all the possible maneuvers could be constructed in real time without any further off-line iteration.

Having achieved the objectives of this study, we also identify the following problem areas which warrant future investigation:

1. The difficulty for solving an optimal maneuver problem with a long control period is greater than solving the same problem with a short control period. Using the same system and boundary conditions, one may solve the short maneuver time problem first and use the resultant trajectory as a starting solution to solve the optimal control problems with long maneuver times.

2. A desirable modification of the iteration methods would be to include hard constraints on the state and control variables, under which the design function of a dynamical system can be executed.

3. In the search for better and more reliable numerical methods, other combination of the methods should be investigated and compared with currently reported methods.

4. A practical extension of the dynamical model would be to consider flexible structures, such as booms, solar panels, and antennas, attached to a rigid spacecraft. Also, the problems of optimal attitude control of a large flexible space station may be considered using the iteration methods to solve for the fundamental rigid body motion and the guidance scheme to control the higher-order perturbed motions due to structure deflections.

5. To consider the torque function more realistically, a modification of the torque function should include smooth rise and fall profiles, tending to minimize structural excitation.

6. The minimum-time maneuver is a challenging topic in the optimal control field, especially for the attitude maneuver problems that are governed by a large set of constrained differential equations.

REFERENCES

1. *Spacecraft Attitude Determination and Control*, edited by J. R. Wertz, D. Reidel Publishing Company, Boston, 1978.

2. Baumann, W. T., "Feedback Control of Multiinput Nonlinear Systems by Extended Linearization," IEEE Transactions on Automatic Control, Vol. 33, No. 2, February 1988, pp. 193-197.

3. Salehi, S. V. and Ryan, E. P., "Optimal Non-Linear Feedback Regulation of Spacecraft Angular Momentum," Optimal Control Applications and Methods, Vol. 5, 1984, pp. 101-110.

4. Wie, B. and Barba, P. M., "Quaternion Feedback for Spacecraft Large Angle Maneuvers," Journal of Guidance, Control, and Dynamics, Vol. 8, No. 3, May-June 1985, pp. 360-365.

5. Dabbous, T. E. and Ahmed, N. U., "Nonlinear Optimal Feedback Regulation of Satellite Angular Momenta," IEEE Transaction on Aerospace and Electronic Systems, Vol. AES-18, No. 1, January 1982, pp. 2-10.

6. Dwyer, T. A. W., "Exact Nonlinear Control of Large Angle Rotational Maneuvers," IEEE Transactions on Automatic Control, Vol. AC-29, No. 9, September 1984, pp. 769-774.

7. Carrington, C. K. and Junkins, J. L., "Optimal Nonlinear Feedback Control for Spacecraft Attitude Maneuvers" Journal of Guidance, Control, and Dynamics, Vol. 9, No. 1, January-February 1986, pp. 99-107.

8. Junkins, J. L. and Turner, J. D., "Optimal Continuous Torque Attitude Maneuvers," Journal of Guidance, Control, and Dynamics, Vol. 3, No. 3, May-June 1980, pp. 210-217.

9. Skaar, S. B. and Kraige, L. G., "Large-Angle Spacecraft Attitude Maneuvers Using an Optimal Reaction Wheel Power Criterion," The Journal of the Astronautical Sciences, Vol. 32, No. 1., January-March, 1984, pp. 47-61.

10. Sidar, M., "An Iterative Algorithm for Optimal Control Problems," International Journal of Non-Linear Mechanics, Vol. 3, 1968, pp. 1-6.

11. Vadali, S. R., "Solution of the Two-Point Boundary Value Problems of Optimal Spacecraft Rotational Maneuvers," Ph. D. Dissertation, VPI & SU, December 1982.

12. Hales, K. A., Flügge-Lotz, I., and Lange, B. O., "Minimum-Fuel Attitude Control of a Spacecraft by an Extended Method of Steepest-Descent," International Journal of Non-Linear Mechanics, Vol. 3, 1968, pp. 413-437.

13. Wolske, G. D., "Minimum Fuel Attitude Control of A Non-Linear Satellite System," International Journal of Non-Linear Mechanics, Vol. 5, 1970, pp. 557-579.

14. Thompson, R. C., "Solution of Two-Point Boundary Value Problems in Optimal Maneuvers of Flexible Vehicles," Ph. D. dissertation, VPI & SU, November 1987.

15. Lin, Y. Y. and Kraige, L. G., "Enhanced Techniques for Solving The Two-Point Boundary-Value Problem Associated with the Optimal Attitude Control of Spacecraft," to appear in The Journal of the Astronautical Sciences.

16. Bryson, A. E., Jr. and Ho, Y. C., *Applied Optimal Control*, Halsted Press, Washington, D. C., 1975.

17. Tolle, H., *Optimization Methods*, Springer-Verlag, New York, 1975.

18. Leitmann, G., *An Introduction to Optimal Control and Calculus of Variations*, Plenum Press, New York, 1981.

19. Kelley, H. J., "Methods of Gradients," Chapter 6, pp. 205-254 of *Optimization Techniques with Applications to Aerospace System*, edited by G. Leitmann, Academic Press, New York, 1962.

20. Merriam III, C. W., *Optimization Theory and the Design of Feedback Control Systems*, McGraw-Hill, New York, 1964.

21. Fletcher, R., *Practical Methods of Optimization Vol. 1*, John Wiley and Sons, New York, 1980.

22. Scales, L. E., *Introduction to Non-Linear Optimization*, Springer-Verlag, New York, 1985.

23. Kopp, R. E. and McGill, R., "Several Trajectory Optimization Techniques Part I: Discussion," pp. 65-89 of *Computing Methods in Optimization Problems*, edited by A. V. Balakrishnan and L. W. Neustadt, Academic Press, London, 1964.

24. Hestenes, M., *Conjugate Direction Methods in Optimization*, Springer-Verlag, New York, 1980.

25. Lasdon, L. S., Mitter, S. K., and Warren, A. D., "The Method of Conjugate Gradients for Optimal Control Problems," IEEE Transactions on Automatic Control, Vol. AC-12, No. 2, April 1967, pp. 132-138.

26. Miele, A. and Iyer, R. R., "General Technique for Solving Nonlinear Two-Point Boundary-Value Problems Via the Method of Particular Solutions," Journal of Optimization Theory and Applications, Vol. 5, No. 5, 1970.

27. Denn, M. M., *Optimization by Variational Methods*, Robert E. Krieger Publishing Company, Huntington, New York, 1978.

28. Blank, D. and Shinar, J., "Efficient Combinations of Numerical Techniques Applied for Aircraft Turning Performance Optimization," Journal of Guidance, Control, and Dynamics, Vol. 5, No. 2, March-April 1982, pp. 124-130.

29. Quinney, D., *An Introduction to the Numerical Solution of Differential Equations-Revised Edition*, Research Studies Press, England, 1987.

30. Gill, P. E., Murray, W., and Wright, M. H., *Practical Optimization*, Academic Press, New York, 1981.

31. Pierre, D. A., *Optimization Theory with Applications*, John Wiley & Sons, New York, 1969.

32. Junkins, J. L. and Turner, J. D., *Optimal Spacecraft Rotational Maneuvers*, Elsevier Science Publishing Company, New York, 1986.

33. Hughes, P. C., *Spacecraft Attitude Dynamics*, John Wiley & Sons, New York, 1986.

34. Kane, T. R., *Spacecraft Dynamics*, McGraw-Hill, New York, 1983.

35. Junkins, J. L., Morton, H. S. Jr., Kraige, L. G., and Blanton, J. N., "Derivation of the Rotational Equations of Motion For a Rigid Body with N Symmetric Rotos," report notes, UVA, 1975.

36. Vadali, S. R., Kraige, L. G., and Junkins, J. L., "New Results on the Optimal Spacecraft Attitude Maneuver Problems," Journal of Guidance, Control, and Dynamics, Vol. 7, No. 3, May-June 1984, pp. 378-380.

37. Lee, E. B. and Markus, L., *Foundations of Optimal Control Theory*, John Wiley & Sons, New York, 1967.

38. Kraige, L. G., and Junkins, J. L., "Concept Evaluation for Electro-Optical Stereo Mapping Systems," VPI&SU Final Report, April, 1982.

39. Cruz, J. B., Jr., "Near-Optimal Feedback Control," Chapter 6, pp. 183-240 of *Feedback Systems*, edited by J. B. Cruz, Jr., McGraw-Hill, New York, 1972.

40. Citron, S. J., *Elements of Optimal Control*, Holt, Rinnehart and Winston, New York, 1969.

41. Pesch, H. J., "Numerical Computation of Neighboring Optimum Feedback Control Schemes in Real-Time," Applied Mathematics and Optimization, Vol. 5, 1979, pp. 231-252.

42. Kelley, H. J., "An Optimal Guidance Approximation Theory," IEEE Transactions on Automatic Control, Vol. AC-9, October 1964, pp. 375-380.

43. Breakwell, J. V., Speyer, J. L., and Bryson, A. E., "Optimization and Control of Nonlinear Systems Using the Second Variation," Journal of Society Industrial and Applied Mathematics in Control, Ser. A, Vol. 1, No. 2, 1963, pp. 193-223.

44. Breakwell, J. V. and Ho, Y. C., "On the Conjugate Point Condition for the Control Problem," International Journal of Engineering Science, Vol. 2, No. 6, March 1965, pp. 565-579.

45. Lee, I., "Optimal Trajectory, Guidance, and Conjugate Points," Information and Control, Vol. 8, No. 6, December 1965, pp. 589-606.

46. Pesch, H. J., "Numerical Computation of Neighboring Optimal Feedback Control Schemes in Real-Time," Applied Mathematics and Optimization, Vol. 5, 1979, pp. 231-252.

The vita has been removed from the scanned document